



ELSEVIER

available at www.sciencedirect.comjournal homepage: www.elsevier.com/locate/cortex

Research report

Altered effective connectivity and anomalous anatomy in the basal ganglia-thalamocortical circuit of stuttering speakers

Chunming Lu^a, Danling Peng^{a,*}, Chuansheng Chen^b, Ning Ning^{a,c}, Guosheng Ding^a, Kuncheng Li^d, Yanhui Yang^d and Chunlan Lin^e

^aState Key Laboratory of Cognitive Neuroscience and Learning, Beijing Normal University, Beijing, China

^bDepartment of Psychology and Social Behavior, University of California, Irvine, CA, USA

^cDepartment of Psychology, School of Education, Suzhou University, Suzhou, China

^dDepartment of Radiology, Xuanwu Hospital, Capital University of Medical Sciences, Beijing, China

^eStuttering Therapy Center, Beijing, China

ARTICLE INFO

Article history:

Received 7 October 2008

Reviewed 19 November 2008

Revised 24 December 2008

Accepted 21 February 2009

Action editor Stefano Cappa

Published online ■

Keywords:

Stuttering

SEM

VBM

Effective connectivity

ABSTRACT

Combining structural equation modeling (SEM) and voxel-based morphometry (VBM), this study investigated the interactions among neural structures in the basal ganglia-thalamocortical circuit (BGTC) in the left hemisphere of stuttering and non-stuttering speakers. Stuttering speakers ($n = 12$) and non-stuttering controls ($n = 12$) were scanned while performing a picture-naming task and a passive-viewing (baseline) task. Results showed significant differences between stuttering and non-stuttering speakers in both effective connectivity and anatomical structures in the BGTC in the left brain. Specifically, compared to non-stuttering speakers, stuttering speakers showed weaker negative connectivity from the left posterior middle temporal gyrus (PMTG) to the putamen, but stronger positive connectivity from the putamen to the thalamus, from the thalamus to the PMTG and anterior supplementary motor area (preSMA), and from the anterior superior temporal gyrus (ASTG) to the preSMA. Accompanying such altered connectivity were anatomical differences: compared to non-stuttering controls, stuttering speakers showed more grey matter (GM) volume concentration in the left putamen, less GM volume concentration in the left medial frontal gyrus and ASTG, and less white matter volume concentration underlying the left posterior superior temporal gyrus inside the BGTC. These results shed significant light on the neural mechanisms (in terms of both functional connectivity and neural anatomy) of stuttering.

© 2009 Published by Elsevier Srl.

1. Introduction

Stuttered speech is characterized by frequent repetition or prolongation of sounds or syllables or words, or frequent

hesitations or pauses. When stuttering is severe enough to markedly disrupt the rhythmic flow of speech and persists for an extended period (e.g., more than three months), it is considered a disorder (WHO, 2007, ICD-10). It is estimated that

* Corresponding author. State Key Laboratory of Cognitive Neuroscience and Learning, Beijing Normal University, 19 Xijiekouwai Street, Beijing 100875, China.

E-mail addresses: luchunming@bnu.edu.cn (C. Lu), pdl3507@bnu.edu.cn (D. Peng).

0010-9452/\$ – see front matter © 2009 Published by Elsevier Srl.

doi:10.1016/j.cortex.2009.02.017

about 1% of the general population are afflicted with this disorder (Andrews et al., 1983; Craig and Tran, 2005). Most of them begin stuttering in early childhood, thus suffering from developmental stuttering. A rarer type of stuttering is the acquired or neurogenic stuttering, which occurs typically in adulthood after a neurological trauma such as head injury, tumor, or stroke.

Researchers have long been interested in the neural basis of stuttering, especially developmental stuttering. Because of the hemispheric asymmetry in language processing, early research on stuttering focused on the role of the two hemispheres. Early electroencephalography (EEG) and dichotic listening studies suggest that stuttering speakers tend to have more activity in the right hemisphere of the brain during speech than do non-stuttering speakers (Boberg et al., 1983; Curry and Gregory, 1969; Moore, 1986; Moore and Haynes, 1980). More recent positron emission tomography (PET) and functional magnetic resonance imaging (fMRI) studies have further confirmed these results (e.g., De Nil et al., 2003; Fox et al., 1996, 2000; Neumann et al., 2003; Preibisch et al., 2003; Wu et al., 1995). Although these results may lead one to believe that the right hemisphere is related to stuttering, a now-classic study by Braun et al. (1997) revealed that activation in the right hemisphere was related to *fluent* speech among stuttering speakers, whereas activation in the left hemisphere was related to the production of *stuttered* speech. Based on such evidence, these researchers concluded that the primary dysfunction in stuttering is located in the left hemisphere and that the hyper-activation of the right hemisphere might not be the cause of stuttering, but rather a compensatory process. It is worth noting that the idea of contralateral compensation has long been noted by neurologists. For example, in their 1914 book, Everbusch et al. discussed the brain and aphasia and wrote “the right hemisphere easily vicariates for the left in childhood” (Everbusch et al., 1914, p. 461).

Braun et al.’s (1997) conclusion is also consistent with the most recent data on the structural differences in the brain between stuttering children and adults. Among stuttering children, anatomical abnormality is found in the left hemisphere (Chang et al., 2008), whereas among stuttering adults, many anatomical abnormalities are evident in the right hemisphere (Jäncke et al., 2004). It appears that anatomical abnormality in the left hemisphere is responsible for stuttering, but a lifetime of stuttering can also lead to changes in the compensatory areas in the contralateral (right) hemisphere (Chang et al., 2008). Based on these results, the present study focused on the functional and structural abnormality in the left hemisphere of the stuttering speakers. Furthermore, different from previous research that attempted to localize brain areas related to stuttering, the present study investigated the (dys)functional interactions among those areas because stuttering is most likely to be a problem of communications among widely distributed brain areas that constitute a dynamic neural system for speech production.

There is an emerging consensus that the basal ganglia-thalamocortical circuit (BGTC) (see Fig. 1) is the neural network involved in stuttering. Previous research showed that stuttering and non-stuttering speakers differ significantly in activation patterns in the BGTC, especially in the left frontal

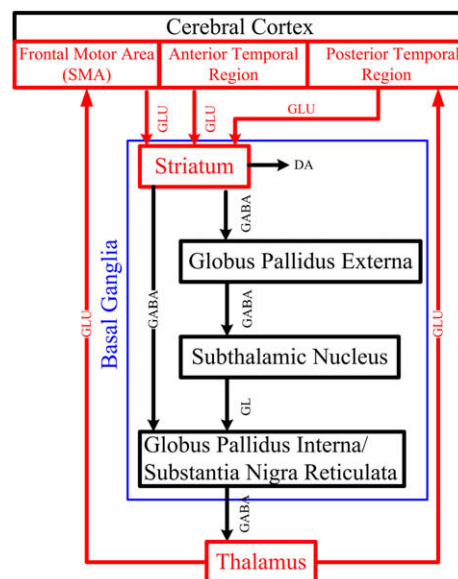


Fig. 1 – Schematic illustration of the BGTC (Alexander et al., 1986, from Honey et al., 2003). The excitatory afferent projections of the striatum originate from the cerebral cortex. Output from the striatum goes to the thalamus by either a direct or an indirect route. It finally returns to the cerebral cortical areas that issue the original efferent projection to the basal ganglia. The red parts of the model were examined in the present study. DA = dopamine; GLU = glutamate; GL = glutamine; GABA = γ -amino butyric acid.

motor cortex, the temporal cortex, and the basal ganglia (e.g., Braun et al., 1997; Brown et al., 2005; De Nil et al., 2003; Fox et al., 1996; Giraud et al., 2008; Ingham et al., 2000). Within the frontal motor cortex, the supplementary motor area (SMA, including both the SMA proper and anterior supplementary motor area – preSMA) may play a special role. Many studies have shown a close relation between the SMA and stuttering (see Abe et al., 1993; Alm, 2004; Packman et al., 2007). Although previous studies on stuttering did not focus on the differences between the SMA proper and preSMA (e.g., Braun et al., 1997; Fox et al., 2000; Ingham et al., 2000), the preSMA, along with the basal ganglia, seems to have a closer relation with syllable representation and spatially and temporally serial coordination of motor apparatus than does the SMA proper (e.g., Alario et al., 2006; Bohland and Guenther, 2006; Crosson et al., 2001; Ferrandez et al., 2003; Hikosaka et al., 1996; Lewis et al., 2004). The preSMA ($y > 0$) was also reported to be positively correlated with stuttering rate and to show deactivation during reading as compared with resting in stuttering speakers (Fox et al., 2000; Ingham et al., 2000). In sum, the preSMA seems to be an important component of the dysfunctional neural system in stuttering.

In terms of the role of the temporal cortex in stuttering, a recent meta-analysis showed under-activation in a part of the superior temporal sulcus located just anterior to those areas that had been found to have voice-selective auditory representations (Brown et al., 2005). In contrast, the posterior part of the temporal cortex appeared to be activated only in

stuttering speakers ($y = -24$) (Brown et al., 2005). These results suggest that the anterior and posterior parts of the temporal cortex may play different roles in the primary dysfunction of the left hemisphere of stuttering speakers. In fact, possible differential roles of the posterior and anterior parts of the temporal cortex in speech and speech-like information processing have also been documented among normal subjects (e.g., Rauschecker and Tian, 2003; Scott et al., 2000; Specht and Reul, 2003).

Finally, the basal ganglia are an important component of the neural network involved in stuttering because they modulate the activity of the left motor and temporal cortices (Alexander et al., 1986; Kolomiets et al., 2003; Saint-Cyr, 2003; Takada et al., 1998a, 1998b). Anatomically, the largest contingent of afferents of the basal ganglia comes from almost the entire cerebral cortex, and the efferent connections are projected to the cerebral cortex through the thalamus (Brodal, 2004). Functionally, the basal ganglia-related circuits are involved in sequence learning by providing internal timing cues (e.g., Cunnington et al., 1996; McFarland and Haber, 2002). The critical role of the basal ganglia in stuttering was recently delineated in an extensive review (Alm, 2004).

To summarize, the BGTC (including the basal ganglia-thalamus, frontal cortex, and temporal cortex) seems to be likely neural correlates of the left hemisphere's dysfunction among stuttering speakers. Furthermore, researchers (e.g., Ludlow and Loucks, 2003) believe that the central control abnormalities in stuttering are not due to disturbance in one or another of the above particular brain regions but rather dysfunctional interactions that interfere with rapid and dynamic speech processing for production. In fact, several studies have examined the dysfunctional interactions among brain areas in the left hemisphere. For example, using the magnetoencephalography (MEG) technique, Salmelin et al. (2000) found that stuttering speakers showed dysfunctional interactions among the inferior frontal cortex, the motor/premotor cortex, and other sylvian regions. In a diffusion tensor imaging (DTI) study, Sommer et al. (2002) found that diffusion characteristics of the group with persistent developmental stuttering and controls differed significantly immediately below the laryngeal and tongue representation in the left sensorimotor cortex. Although these studies revealed dysfunctional interactions among brain regions in stuttering speakers, neither of them focused on brain connectivity. To our knowledge, no studies have used connectivity analysis to directly examine the interactions among brain regions in stuttering. Connectivity analysis is helpful in testing how the different regions involved in stuttering are functionally connected to one another and how such connection may or may not differ between stuttering and non-stuttering speakers. In the present study, we used the structural equation modeling (SEM) technique to explore how the nodes of the BGTC interacted with one another in stuttering and non-stuttering speakers (see Fig. 1).

Since its introduction by McIntosh et al. (1994), neural connectivity analysis has been used in a wide range of functional MRI studies (e.g., Büchel and Friston, 1997; Doeller et al., 2006; Fu et al., 2006; Goncalves et al., 2001; Honey et al., 2003; Iidaka et al., 2006; Schlosser et al., 2006; Zhuang et al., 2005). Several multivariate techniques have been employed

to investigate effective connectivity. One of them is the SEM, which was originally developed in social sciences to examine causal relations among latent (unobserved) variables. When used to analyze imaging data, SEM is synonymous with path analysis, which includes only observed variables. It combines an *a priori* anatomically plausible (constraining) model and the inter-regional covariance of activity (McIntosh and Gonzalez-Lima, 1994a, 1994b). For any given model, SEM estimates a set of free parameters (connection weights and residual variances) that could reproduce a covariance matrix as closely as possible to the sample covariance matrix. Statistical inference about the model is made based on discrepancy measures (e.g., maximum likelihood function) between the covariance matrix reproduced by the model and the sample covariance matrix (Bullmore et al., 2000). The resulting parameters are estimates of effective connectivity. When standardized coefficients are used, the parameters represent the magnitude of response (in units of standard deviations) of one brain region to another, while activity in other regions included in the model is held constant (Büchel et al., 1999). SEM also allows for group comparisons of the estimated parameters (Della-Maggiore et al., 2000; McIntosh, 1999).

In addition to the effective connectivity analysis, we further investigated whether dysfunctional connections (if they were found) might have been accompanied by anomalous anatomy. Atypical cerebral structures have been reported among developmental stuttering speakers, but the results are inconsistent. Employing different methods, Foundas et al. (2001) and Sommer et al. (2002) reported different kinds of anomalous cerebral structures. No single anatomic feature distinguished the stuttering and the non-stuttering groups. They seemed to differ in multiple loci within a widely distributed neural network (Foundas et al., 2001). Guided by previous findings in the literature, the present study used voxel-based morphometry (VBM) to look for evidence of anomalous brain structures in specific regions where SEM had shown dysfunctional connectivity.

2. Experimental procedures

2.1. Participants

Twelve stuttering subjects (10 males and 2 females; mean age = 24.5 years, ranging from 19 to 31 years), and 12 non-stuttering controls (8 males and 4 females; mean age = 24 years, ranging from 22 to 29 years) were recruited for this study (see Table 1). Data from ten stuttering (9 males and 1 female) and nine of the non-stuttering subjects (5 males and 4 females) were used in the SEM analysis and data from all twelve stuttering and twelve non-stuttering subjects were used in the VBM analysis. The reason for the varying sample sizes for different analyses was that three non-stuttering subjects and two stuttering subjects did not finish the scanning session, so their functional imaging data were not used, but their anatomical imaging data were used in the VBM analysis. Stuttering subjects were selected from a waiting list at the Stuttering Therapy Center of Beijing, China. All of the stuttering subjects began their stuttering during

Table 1 – Subjects' information.

| | | Stuttering subjects | | | Non-stuttering subjects | |
|--|--------|--------------------------|-----------|------------------------|-------------------------|-----------------|
| Number | | 12 | | | 12 | |
| Male:Female | | 10:2 | | | 8:4 | |
| Chronological age (years) | | 24.5 (19–31) | | | 24 (22–29) | |
| Educational level (years) | | 17 (15–19) | | | 15.5 (16–19) | |
| Detailed information about stuttering subjects | | | | | | |
| ID | Gender | Handedness (± 100) | Severity | SSI score (percentile) | Age of onset (years) | Treatment |
| S1 | M | R (100) | Very mild | 13 (5) | <12 | Y (4 years ago) |
| S2 | M | R (100) | Very mild | 15 (8) | <4 | Y (3 years ago) |
| S3 | M | R (90) | Mild | 21 (24) | <5 | N |
| S4 | M | R (75) | Mild | 22 (28) | <12 | Y (1 year ago) |
| S5 | M | R (90) | Mild | 23 (36) | <7 | N |
| S6 | M | R (78) | Mild | 24 (40) | <4 | N |
| S7 | M | R (100) | Moderate | 27 (60) | <10 | N |
| S8 | F | R (100) | Moderate | 28 (61) | <11 | N |
| S9 | M | R (100) | Moderate | 29 (65) | <4 | Y (3 years ago) |
| S11 | F | R (100) | Severe | 33 (81) | <3 | N |
| S10 | M | R (90) | Severe | 35 (89) | <8 | N |
| S12 ^a | M | R (100) | | | <4 | N |

M, male, F, female, Y = Yes, N = No, "<" means "earlier than".
^a The detailed information about stuttering severity of S12 was accidentally lost.

childhood (prior to the age of 12 years). Only four subjects had ever received any kind of treatment, but none of them received treatment during the year prior to this study. Their symptoms were diagnosed as ranging from very mild to severe ($M = 24.55$, $S.D. = 6.82$) according to the Stuttering Severity Instrument (SSI)-III (Riley, 1994). SSI-III was administered by two independent therapists, and the inter-rater reliability between them was high (Cronbach $\alpha = .94$). All subjects reported no neurological or language problems except for stuttering.

Non-stuttering subjects were recruited through advertisements. These non-stuttering controls were matched with stuttering subjects in chronological age and educational level. They reported to have never had any language disorders or neurological diseases.

All subjects were right-handed, native Chinese speakers. Hand preference was assessed by a computerized program of the Edinburgh Handedness Inventory with a cutoff of +40 (right handedness) (Oldfield, 1971). All subjects gave written informed consent for their participation in this study.

2.2. Tasks and materials

Subjects were scanned while performing a picture-naming task and a passive-viewing (baseline) task. The pictures were standard simple line drawings of common objects selected from a standardized picture database (Zhang and Yang, 2003). All of these pictures had a similar level of conceptual familiarity, visual complexity, and semantic difficulty based on the ratings of 30 subjects not involved in the present study. Every picture had a common Chinese name that is three characters long. The pictures in the baseline condition were nonsense pictures formed by randomizing the pixels of the pictures in the naming condition to ensure comparable overall

luminance. These unnamable baseline pictures were used to control for the primary visual processing.

There was one run in the experiment. After the machine was stabilized, subjects were presented with the baseline task (i.e., 8–12 nonsense pictures in a random order) for 24–36 sec. Following the baseline task was the naming task (8–12 pictures, again, presented in a random order), which lasted for 24–36 sec. There were 6 blocks of the baseline task and 6 blocks of the naming task. There were a total of 132 trials, each lasting for 3000 msec (total scanning time = 396 sec).

During the experiment, participants lay supine within the magnetic resonance (MR) scanner with their head secured in foam padding. An IBM (International Business Machines Corp.) ThinkPad notebook was used to present stimuli programmed with the Inquisit software [Inquisit 2.0.4.1230 (Computer software), 2004, Seattle, WA: Millisecond Software]. An LCD (liquid crystal display) projector displayed stimuli from inside the MR control room onto a back-projection screen located at the foot of the MR scanner. Participants viewed the stimuli via a mirror attached to the head coil above their eyes.

For each trial, a picture was presented for 1000 msec, followed by a blank screen of 2000 msec. During the picture-naming trials, subjects were asked to name the picture by making minimal movement of their mouth. Both accuracy and speed were emphasized. During the baseline (nonsense picture viewing) trials, subjects were asked to view the randomized pixels without any mouth movement. The verbal responses of the subjects were monitored by a built-in microphone (some of the verbal responses were difficult to assess because of the scanner noise). Stuttering frequency assessment was performed by two experimenters independently. During the production of three-syllable picture names, the following were coded as stuttering events: (a) subjects failed to pronounce the initial phoneme in a syllable or had

great difficulty doing it; (b) the pronunciation of phonemes other than the initial ones was suddenly blocked; (c) the pronunciation of phonemes was involuntarily prolonged; or (d) phonemes or syllables were involuntarily repeated more than two times. Multiple stuttering events that occurred during the naming of the same picture were counted as one event. Among the responses of stuttering speakers that could be clearly differentiated from the noise in the background, most speech was fluent. Because both the verbal responses and the response time data could not be reliably obtained in the scanner due to its high level of noise, they were estimated with the behavioral data collected immediately before the scanning. The same procedure was successfully used in a previous study (Liu et al., 2006).

During behavioral data collection, a fixation was presented for 150 msec, followed by a picture. The picture stayed on the screen until subjects responded or 4500 msec had lapsed. Like the speech during scanning, most of the speech of the stuttering speakers during behavioral data collection was fluent. The following responses were coded as errors (not including the stuttering event): (a) response time that was less than 200 msec or more than 4500 msec; and (b) naming the pictures with a wrong name.

2.3. Imaging parameters

Functional and anatomical images were collected with a 1.5 T whole-body Siemens Magnetom Sonata Meastro Class scanner (Siemens, Erlangen, Germany) equipped with the standard clinical head coil. Additional padding between the headphone and the head coil was used to restrain the subject's head. Anatomical spin-echo T1-weighted images were acquired for image registration (TR = 500 msec, TE = 14 msec, flip angle = 90°, FOV = 220 mm, matrix = 128 × 128, 20 slices, slice thickness = 6 mm, transversal plane, resolution = 1.8 × 1.8 mm). Functional whole-brain T2*-weighted images were acquired using a single-shot gradient-recalled EPI sequence [TR = 3000 msec; TE = 50 msec; flip angle = 90°; FOV = 220 mm, matrix = 64 × 64 (in-plane resolution = 3.4 × 3.4 mm), 20 slices, slice thickness = 6 mm] with interleaved slice acquisition. For anatomical localization and VBM analysis, standard whole-brain, high-resolution 3D structural images were acquired using a T1-weighted, 3D, MP-RAGE sequence (TR = 1970 msec; TE = 3.93 msec; flip angle = 15°; FOV = 220 mm; matrix = 256 × 256; 96 slices; slice thickness = 1.7 mm, sagittal plane; resolution = .48 × .48 mm).

The software package AFNI (<http://afni.nimh.nih.gov/afni>) was used to pre-process the data in order to prepare for the subsequent SEM analysis (Cox, 1996). The images of the first two time points were discarded to control for haemodynamic delay effects. Slice timing correction, image registration, and motion correction were performed (Cox and Jesmanowicz, 1999). The functional image time series were then smoothed with a low pass filter and Isotropic Gaussian blur (FWHM = 6 mm). Regression coefficients β were obtained by deconvolving the time series using Legendre polynomial fitting method within the general linear model and were then converted into percentage of signal change. Finally, individual images were resampled into Talairach coordinates using the AFNI hand landmarking procedure (resampled

volumes = 1 mm³). Percentage of signal change for task was compared with that of baseline by a one-sample *t* test. Correction for multiple comparisons was achieved by a voxel-cluster threshold technique for an overall corrected level of significance (alpha) of .05 (individual voxel $p < .01$, minimum cluster threshold required = 300 mm³) based on the results of a Monte Carlo simulation at the cluster level (Forman et al., 1995; Xiong et al., 1995). Then, the percentage of signal change was compared voxel-by-voxel between stuttering and non-stuttering speakers with an independent two-sample *t* test. Correction for multiple comparisons was achieved by the same method as above (individual voxel $p < .01$, minimum cluster threshold required = 300 mm³).

2.4. SEM

As mentioned earlier, we used SEM to examine effective connectivity in this study. SEM was selected over other causal modeling techniques such as dynamic causal modeling (DCM) (Friston et al., 2003) for several reasons. First, SEM has a relatively longer history and is more commonly used in the analysis of imaging data. Second, unlike DCM, SEM does not have a strict requirement of a short TR (such as less than 2 sec). Third, several researchers have recently developed useful methods to improve the use of SEM for fMRI data (e.g., Bullmore et al., 2000; Kim et al., 2007; Zhuang et al., 2005).

The first step in SEM analysis of imaging data is to determine the *a priori* anatomically plausible model. This can be accomplished by either the hypothesis-driven or the data-driven approach or more commonly a combination of both approaches. In the present study, we established the *a priori* anatomical model by a combination of the data-driven and hypothesis-driven approaches. First, significant activation clusters were identified by the whole-brain voxel-wise group comparisons mentioned above. The model was then based on those areas that exhibited significant differences in neural activity between stuttering and non-stuttering speakers. Second, although many brain areas showed significant group differences, we only focused on the areas of interest to the BGTC model as described in the Introduction (see Fig. 1). They included the following five left brain regions (with their Talairach coordinates): the putamen, $x, y, z = -25, -3, 14$; thalamus, $x, y, z = -26, -26, -1$; preSMA (BA6), $x, y, z = -12, 1, 56$; anterior temporal cortex (superior temporal gyrus, BA38) (ASTG), $x, y, z = -34, 0, -13$; and posterior temporal cortex (middle temporal gyrus, BA22) (PMTG), $x, y, z = -53, -50, 6$.

Regions were defined as spheres (3 mm radius) centered on the above coordinates. Before the extraction of the time series, individual subject's images were converted into percentage of signal change after being smoothed with a low pass filter and Gaussian blur, and then resampled into Talairach coordinates with the resampled volume of 1 mm³. For each region of interest (ROI), a representative time series was acquired by simply averaging the time series of all voxels within the ROI for each subject. Principal components analysis (PCA) was then used to identify an "average" pattern of responses in each ROI across all subjects (Büchel et al., 1999; Fletcher et al., 1999). PCA was conducted for the stuttering and the non-stuttering subjects separately. This procedure ensured that

each time series accounted for the most variance among subjects for each group of subjects.

LISREL 8.7 was used to run SEM. It used an iterative maximum likelihood algorithm to calculate path coefficients and to achieve the best match between the covariance matrix reproduced by the model and the observed variance–covariance structure from the data (Higham, 1993; Jöreskog and Sorbom, 1996). Derived from the logarithmic expression of a likelihood ratio test, the maximum likelihood (ML) discrepancy function was introduced $F_{ML} = \log|\Sigma(\theta)| + \text{tr}(S\Sigma^{-1}(\theta)) - \log|S| - k$ (Jöreskog, 1967) to indicate the fit of the model. A good model aims to minimize this function. When it reaches a value of 0, it means that the sample covariance matrix S equals the population covariance matrix Σ given a certain parameter vector (θ). The ML discrepancy function yields an overall fit statistic that follows a central χ^2 -distribution under the null hypothesis that the model is correct in the population. In addition to ML discrepancy function, there are other alternative fit indices such as the Root Mean Square Error of Approximation (RMSEA), Comparative Fit Index (CFI), and Parsimony Goodness of Fit Index (PGFI) (Browne and Cudeck, 1993; Steiger and Lind, 1980). They have been used in neuroimaging studies as well (Au Duong et al., 2005; Bentler, 1990; Goncalves et al., 2001; Honey et al., 2003; Schlosser et al., 2006; Zhuang et al., 2005). Besides the overall fit indices, the reported t value for each path coefficient in the model should be greater than a certain critical value to reject the null hypothesis that the coefficient is 0. We used a path coefficient threshold of .05 ($t > 1.98$ and $p < .05$ with a degree of freedom above 60).

When running SEM, one must consider both the anatomy of the brain, as well as the complexity of the model. One of the constraints is that the number of free (i.e., to-be-estimated) parameters cannot exceed a certain number $t = 1/2 \times p \times (p + 1)$ (p is the number of variables). It has been suggested that the residual variance for each variable can be set arbitrarily as from .35 to .40 (McIntosh and Gonzalez-Lima, 1994a), or estimated by the ratio between the first eigenvalue and the sum of eigenvalues in order to increase the number of free path coefficients to be estimated (Bullmore et al., 2000). However, the best method for fitting a model may be to estimate the residual variance freely (Lubke and Dolan, 2003). In the present study, the residual variance was first freely estimated in order to get the appropriate value within the model, and then set as the estimated appropriate value to improve the model fit and path coefficient estimation.

In order to obtain the best-fitting path model, a step-wise method was employed as suggested by Bullmore et al. (2000). That is, the process of model searching started from the worst fitting model—the “null model” in which all path coefficients were constrained or set to zero. The algorithm computed the modification index (MI) or so-called Lagrangian multiplier (LM) for each constrained coefficient and allowed the coefficient with the maximum MI to be nonzero until the index of model fit did not improve significantly.

Statistical inferences about group differences were based on a stacked-models approach. This included a comparison of a free model, in which all connections were allowed to vary between the two groups of subjects, to a restricted model, in which a given connection was forced to be equal for the two groups. First, an omnibus test was applied in which the model

with all parameters constrained to be the same between the two groups was compared with the model without any constraints. This step would show whether any of the paths between the two models were significantly different, but would not specify which of the paths were actually significantly different. The comparison of models was done by subtracting the goodness-of-fit χ^2 value for the constrained model from the χ^2 value for the free model. The difference (χ^2_{diff}) was assessed with the degrees of freedom equal to the difference in the degrees of freedom for the constrained and free models (McIntosh et al., 1994). A significant χ^2_{diff} indicated that at least one path differed significantly across the two groups of subjects (McIntosh and Gonzalez-Lima, 1994a, 1994b). When the omnibus test showed a significant difference between the two groups, the next step was to find specific paths that differed between the two groups. This was done by constraining one path at a time to be the same between the two groups while other paths were unconstrained (to be estimated freely). This model was compared with the model without any constraints by the χ^2_{diff} ($df = 1$) test. A p value of .05 (two-tailed) was chosen as the threshold for significance.

2.5. VBM analysis

The anatomical images were analyzed with the VBM toolbox within SPM5 (Statistical Parametric Mapping, Wellcome Department of Cognitive Neurology, London, UK). Pre-processing of the images was performed slightly differently from the protocol described by Good et al. (2001). Various preprocessing procedures were combined into a single generative model in SPM5 (Ashburner and Friston, 2005). Estimating the model parameters (for a maximum *a posteriori* solution) involves iterated steps of segmentation estimation, bias correction, and warping. This approach provides better results than simple serial applications of each component. Warping of prior images during segmentation makes segmentation more independent from size, position, and shape of prior images.

Specifically, the images were normalized with a modulated normalization method and segmented into grey matter (GM) and white matter (WM) and cerebro-spinal fluid. Bias correction was applied. The resolution of the normalized images was $1 \times 1 \times 1$ mm. A modulated normalization analysis attempted to correct the volumes for regional expansion/shrinkage during spatial normalization, so that the total amount of GM or WM in the modulated GM/WM remained the same as it would have been in the original images. In SPM5, prior probability maps that are relevant to tissue segmentation are warped to the individual brains, making the creation of a customized template unnecessary (Rüsch et al., 2007), especially when the number of subjects is fewer than 20. The bias-corrected images have more uniform intensities within the different types of tissues. Medium hidden Markov random field (HMRF) weighting (.3) approach was applied to provide spatial constraints. Finally, the data were smoothed with FWHM 3 mm (see the manual of SPM5 for more details about the automatic processing steps).

Statistical comparisons between the stuttering and non-stuttering speakers were performed with a voxel-based

independent two-sample *t* test for both the GM and WM (individual voxel $p < .001$, uncorrected; overall $p < .05$, corrected, $k > 45$, Monte Carlo simulation). The analysis included grand mean scaling. Global nuisance effects were accounted for by scaling the images so that they all had the same global value (proportional scaling).

3. Results

3.1. Behavioral data

Significant group differences in response time were found (see Fig. 2). The response latency of non-stuttering subjects was significantly shorter than that of stuttering subjects, $t(22) = -2.443$, $p < .05$. Because the stuttering frequency of stuttering speakers was too low (<1%), it was not included in the analysis. The error rate data also showed that the naming task elicited more errors in stuttering subjects than in non-stuttering controls, Mann–Whitney Test, $z = -2.079$, $p < .05$. These results implied that the speech production system of stuttering speakers may experience more difficulties in a task that required sequential organization of the speech movements than that of non-stuttering controls.

3.2. Imaging data

Table 2 summarizes the neural activations during speech production in stuttering and non-stuttering speakers. For the non-stuttering speakers, activation was evident in the inferior frontal gyrus (BA46), superior temporal gyrus (BA22), and precuneus in the left hemisphere; the cerebellar pyramis of vermis in the right hemisphere; the precentral gyrus (BA6), insula, thalamus, declive of cerebellum in both hemispheres. Overall, there were more areas with significant activations in the left hemisphere than in the right hemisphere in non-stuttering speakers (7 regions vs 4 regions).

For the stuttering group, activation was found in the precuneus (BA7) of the left hemisphere; the medial frontal gyrus

Table 2 – Brain areas that showed significant activations in stuttering and non-stuttering speakers when performing the picture-naming task as compared to the baseline task.

| Brain area | x | y | z | z-Value | Cluster volume |
|--|-----|-----|-----|---------|----------------|
| <i>Non-stuttering speakers</i> | | | | | |
| L_Inferior Frontal Gyrus (BA46) ^a | -34 | 37 | 11 | 4.00 | 239 |
| R_Precentral Gyrus (BA6) | 51 | -8 | 31 | 4.08 | 338 |
| L_Precentral Gyrus (BA6) | -46 | -12 | 33 | 4.47 | 1227 |
| L_Precuneus | -18 | -48 | 40 | 3.88 | 349 |
| L_Superior Temporal Gyrus (BA22) | -60 | -6 | 10 | 3.31 | 727 |
| L_Insula (BA13) | -43 | 6 | 14 | 3.64 | 1153 |
| R_Insula (BA13) ^a | 42 | 6 | 2 | 3.38 | 128 |
| R_Pyramis of Vermis | 3 | -72 | -30 | 4.19 | 1015 |
| L_Declive | -10 | -56 | -14 | 3.72 | 396 |
| R_Declive | 11 | -60 | -13 | 3.60 | 488 |
| R_Thalamus/Pulvinar | 28 | -28 | 5 | 4.43 | 1737 |
| L_Thalamus/Pulvinar | -20 | -32 | 10 | 4.52 | 5583 |
| <i>Stuttering speakers</i> | | | | | |
| R_Medial Frontal Gyrus (BA6) | 12 | 6 | 53 | 4.05 | 2062 |
| L_Precuneus (BA7) | -25 | -50 | 45 | 4.17 | 355 |
| L_Precentral Gyrus (BA6) | -33 | -10 | 49 | 3.73 | 2065 |
| R_Precentral Gyrus (BA6) | 36 | -5 | 34 | 3.27 | 892 |
| R_Middle Temporal Gyrus (BA22) | 61 | -30 | 4 | 3.62 | 371 |
| R_Middle Occipital Gyrus (BA37) | 47 | -61 | -8 | 3.87 | 756 |
| L_Insula (BA13) | -38 | 19 | 8 | 4.59 | 3415 |
| R_Insula (BA13) | 37 | 18 | 8 | 4.71 | 495 |
| R_Lentiform Nucleus | 24 | 12 | 16 | 3.62 | 2024 |
| L_Thalamus | -20 | -21 | 4 | 3.90 | 471 |
| R_Thalamus | 28 | -29 | 8 | 4.04 | 711 |
| R_Cerebellar Tonsil | 21 | -67 | -34 | 3.35 | 655 |
| R_Declive | 22 | -63 | -14 | 4.23 | 3115 |

Note: Activation threshold was $p < .05$, corrected. The coordinates were in LPI orientation of standard Talairach Space. Areas were sorted according to the anatomical lobe.

a Areas that did not survive the threshold of 300 volume.

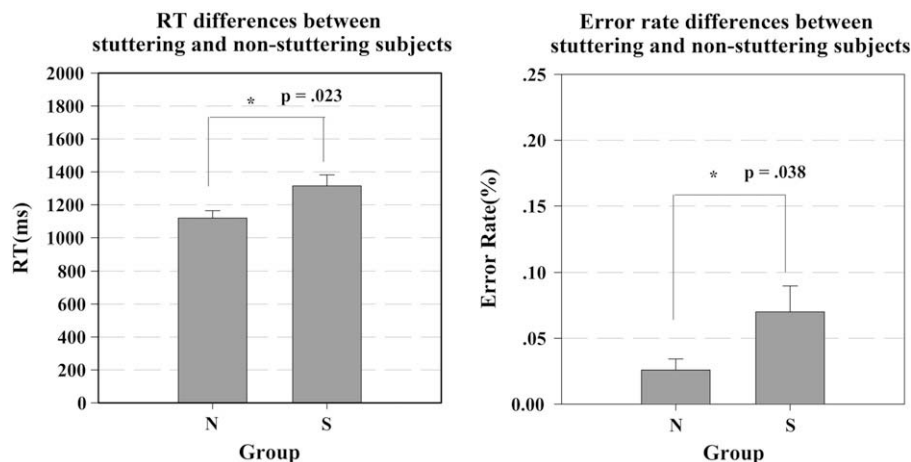


Fig. 2 – Mean response time (RT) and error rate for stuttering and non-stuttering speakers. N, non-stuttering speakers; S, stuttering speakers.

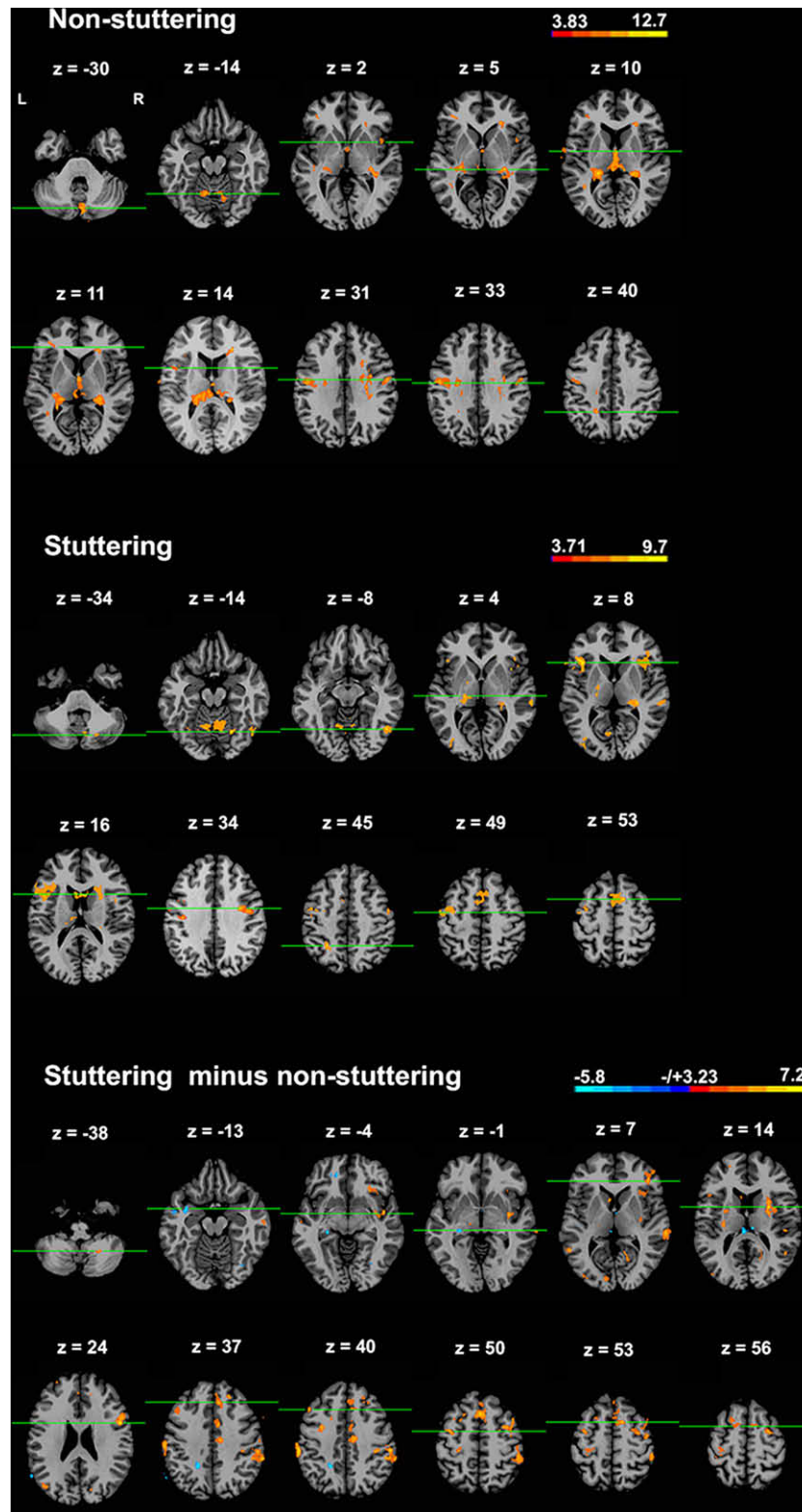


Fig. 3 – Neural activity of the non-stuttering and stuttering speakers during the performance of the picture-naming task as compared to the baseline, and neural differences based on group comparisons between stuttering and non-stuttering speakers when performing the picture-naming task. Gold blobs indicate brain regions that showed more activity among the non-stuttering speakers than the stuttering speakers, and hot blobs indicate brain regions that showed more activity among the stuttering speakers than the non-stuttering speakers.

Table 3 – Brain regions that showed significant group differences between stuttering and non-stuttering speakers when performing the picture-naming task.

| Brain area | x | y | z | z-Value | Cluster volume |
|---|-----|-----|-----|---------|----------------|
| <i>Stuttering speakers > non-stuttering speakers</i> | | | | | |
| R_Superior Frontal Gyrus (BA9) | 20 | 37 | 36 | 3.85 | 307 |
| L_Middle Frontal Gyrus (BA9) | -44 | 21 | 40 | 3.58 | 421 |
| R_Middle Frontal Gyrus (BA6) | 31 | 0 | 49 | 3.97 | 1470 |
| L_Medial Frontal Gyrus (BA6) | -12 | 1 | 56 | 3.00 | 1093 |
| R_Medial Frontal Gyrus (BA6) | 12 | 6 | 53 | 4.01 | 1391 |
| R_Medial Frontal Gyrus (BA6) | 7 | 30 | 37 | 3.30 | 723 |
| R_Inferior Frontal Gyrus (BA44) | 49 | 5 | 24 | 4.77 | 2493 |
| R_Inferior Frontal Gyrus (BA46) | 41 | 33 | 7 | 3.55 | 469 |
| L_Precentral Gyrus (BA6) | -35 | -5 | 50 | 3.80 | 814 |
| L_Postcentral Gyrus (BA1) | -56 | -26 | 39 | 4.41 | 680 |
| R_Postcentral Gyrus (BA2) | 54 | -28 | 39 | 4.27 | 2505 |
| R_Superior Temporal Gyrus (BA42) | 62 | -29 | 6 | 3.91 | 802 |
| L_Middle Temporal Gyrus (BA22) | -53 | -50 | 6 | 3.50 | 386 |
| R_Insula (BA13) | 43 | -6 | -4 | 3.69 | 523 |
| R_Insula (BA13) | 35 | 19 | 7 | 2.99 | 444 |
| L_Putamen | -25 | -3 | 14 | 3.30 | 345 |
| R_Putamen | 27 | 2 | 14 | 4.12 | 880 |
| R_Cerebellar Tonsil ^a | 23 | -51 | -38 | 3.43 | 118 |
| <i>Non-stuttering speakers > Stuttering speakers</i> | | | | | |
| L_Superior Temporal Gyrus (BA38) | -34 | 0 | -13 | -3.46 | 344 |
| L_Thalamus | -26 | -26 | -1 | -3.56 | 619 |

Note: Activation threshold was $p < .05$, corrected. The coordinates were in LPI orientation of standard Talairach Space. Areas were sorted according to the anatomical lobe.
a Areas that did not survive the threshold of 300 volume.

(BA6), middle temporal gyrus (BA22), fusiform gyrus (BA37), lentiform nucleus, declive of cerebellum, and cerebellar tonsil in the right hemisphere; the precentral gyrus (BA6), insula (BA13), and thalamus in both hemispheres. Activations in the right hemisphere were more widespread than in the left hemisphere in stuttering speakers (8 regions vs 4 regions).

Fig. 3 and Table 3 illustrate the brain areas that exhibited different neural activity between stuttering and non-stuttering speakers. Consistent with previous results, these areas were widely distributed (e.g., De Nil et al., 2000; Ingham et al., 2003; Neumann et al., 2003). Specifically, compared to non-stuttering speakers, stuttering speakers showed increased activity in the middle frontal gyrus (BA9), precentral gyrus (BA6), and PMTG (BA22) in the left hemisphere; the superior frontal gyrus (BA9), middle frontal gyrus (BA6), inferior frontal gyrus (BA44/46), superior temporal gyrus (BA42), insula, and cerebellar tonsil in the right hemisphere; and the medial frontal gyrus (BA6), postcentral gyrus (BA1/2), and putamen in both hemispheres. A decrease of activity in stuttering speakers was apparent in the left ASTG (BA38) and left thalamus.

In terms of brain areas in the left hemisphere as specified in the SEM model, stuttering and non-stuttering speakers showed significant differences in activation patterns in all areas, i.e., the putamen, thalamus, ASTG, PMTG, and preSMA. Importantly, there were different patterns of group differences in the ASTG and PMTG: stuttering subjects exhibited less activation in the ASTG, but greater activation in the PMTG, than did non-stuttering subjects.

3.3. Effective connectivity

By using the step-wise method to search for the best model, we found a model that best fit the data of both non-stuttering speakers ($\chi^2 = 2.46$, $df = 6$, $p = .87$; RMSEA = 0 [90% confidence interval - CI (0, .058)]; PGFI = .40, CFI = 1) and stuttering speakers ($\chi^2 = 3.67$, $df = 6$, $p = .72$; RMSEA = 0 [90% CI (0, .084)]; PGFI = .40, CFI = 1). This model is shown in Fig. 4A. The standardized path coefficients for the best-fitting model are presented in Table 4. For non-stuttering subjects, all path

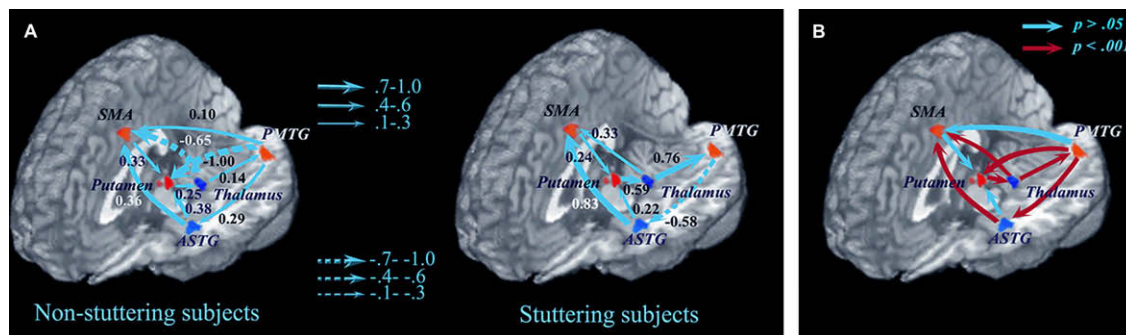


Fig. 4 – A. The best-fitting model for the data from non-stuttering and stuttering speakers. The arrows show directional inter-regional effective connections within the BGTC (solid and dashed arrows for positive and negative connections, respectively). **B.** Results of comparisons for individual path coefficients (blue arrows = not significantly different; red arrows = significantly different). ASTG, left anterior superior temporal gyrus; PMTG, left posterior middle temporal gyrus; preSMA, left anterior supplementary motor area; PUTA, putamen; THAL, left thalamus.

Table 4 – Standardized path coefficients and results of group comparisons based on the best-fitting model of stuttering speakers and non-stuttering controls.

| | Non-stuttering speakers | | Stuttering speakers | | Group comparison | |
|-------------|--------------------------------|--------|--------------------------------|-------|------------------|-------------|
| | Standardized path coefficients | t | Standardized path coefficients | t | χ^2 | p |
| ASTG–preSMA | .36 | 5.00 | .83 | 17.94 | 156.07 | $p < .0001$ |
| ASTG–PUTA | .38 | 5.23 | .22 | 4.28 | 3.37 | $p > .05$ |
| PMTG–ASTG | .29 | 6.12 | –.58 | –3.64 | 38.39 | $p < .0001$ |
| PMTG–preSMA | .10 | 2.26 | –.10 | –.64 | 1.54 | $p > .05$ |
| PMTG–PUTA | –1.00 | –22.70 | –.06 | –.59 | 28.96 | $p < .0001$ |
| preSMA–PUTA | .33 | 2.73 | .24 | 2.24 | .08 | $p > .05$ |
| PUTA–THAL | .25 | 1.60 | .59 | 5.70 | 5.29 | $p < .05$ |
| THAL–PMTG | .14 | 1.38 | .76 | 7.15 | 4.80 | $p < .05$ |
| THAL–preSMA | –.65 | –7.55 | .33 | 3.31 | 88.97 | $p < .0001$ |

Note: Bold numbers indicate a significance level of $p < .05$. ASTG, left anterior superior temporal gyrus; PMTG, left posterior middle temporal gyrus; preSMA, left anterior supplementary motor area; PUTA, left putamen; THAL, left thalamus.

coefficients reached statistical significance at $p < .05$ level except the path from the thalamus to the PMTG ($t = 1.38$). For stuttering subjects, except the paths from the PMTG to the putamen and SMA ($t = -.64$; $t = -.59$, respectively), all other connections were statistically significant at $p < .05$.

The omnibus test indicated that there were significant differences in path coefficients between stuttering and non-stuttering speakers ($\chi^2_{diff} = 573.32$, $df = 12$, $p < .0001$). Tests of individual path coefficients showed that, within the three input sources of the putamen, the negative input from the PMTG was significantly stronger in non-stuttering speakers than in stuttering speakers ($\chi^2_{diff} = 28.96$, $df = 1$, $p < .0001$), whereas the positive input from the ASTG and preSMA to the putamen was not significantly different between the two groups ($\chi^2_{diff} = 3.37$, $df = 1$, $p > .05$; $\chi^2_{diff} = .08$, $df = 1$, $p > .05$) (see Fig. 4B and Table 4). Correspondingly, group differences were also significant in the positive output from the putamen to the thalamus ($\chi^2_{diff} = 5.29$, $df = 1$, $p < .05$) and from the thalamus to the PMTG ($\chi^2_{diff} = 4.80$, $df = 1$, $p < .05$). They were stronger in stuttering speakers than in non-stuttering speakers. The negative projection from the thalamus to the preSMA ($\chi^2_{diff} = 88.97$, $df = 1$, $p < .0001$) in non-stuttering speakers also significantly differed from the positive projection in stuttering speakers. The connection from the PMTG to the ASTG was positive in non-stuttering speakers, and was significantly different from the negative connection in stuttering speakers ($\chi^2_{diff} = 38.39$, $df = 1$, $p < .0001$). Finally, stuttering speakers showed a stronger positive connection from the ASTG to the preSMA than did non-stuttering speakers ($\chi^2_{diff} = 156.07$, $df = 1$, $p < .0001$).

3.4. VBM

The VBM analysis was used to examine whether the dysfunctional connections between brain regions for stuttering speakers were accompanied by anatomical changes or abnormalities. Fig. 5 and Table 5 show the brain regions that differed significantly in WM and GM volume concentration between stuttering and non-stuttering speakers.

Compared to non-stuttering speakers, stuttering speakers showed increased GM volume concentration in the right medial frontal gyri (BA6/32), bilateral precentral gyri (BA6), left

superior parietal lobule (BA7) and paracentral lobule (BA5), right fusiform gyri (BA37), left middle occipital gyri (BA18), bilateral cingulate gyri (BA31/23), and left putamen, but decreased GM volume concentration in the left superior frontal gyrus (BA8), bilateral medial frontal gyri (BA9/10/11), left superior temporal gyrus (BA21), right middle temporal gyrus (BA39), and right cerebellum.

In terms of WM volume concentration, stuttering speakers showed more concentration in areas underlying the right superior frontal gyrus (BA9), left precuneus (BA7), right inferior and superior temporal gyri (BA20/39), and left cerebellum. Stuttering speakers showed less concentration in the right precentral gyrus (BA6), left superior temporal gyrus (BA41), bilateral fusiform gyri (BA37), left lingual gyrus (BA18), and bilateral cerebellum.

4. Discussion

Previous research has documented both functional and anatomical differences in certain regions of the brain between stuttering and non-stuttering speakers (Brown et al., 2005; Chang et al., 2008; Jäncke et al., 2004). Little is known, however, about effective connectivity among these regions in relation to stuttering. By combining the SEM and the VBM methods, the present study provided direct evidence for the dysfunctional interactions between brain regions in stuttering speakers. In the following paragraphs, we will first discuss briefly our results on activation patterns for stuttering and non-stuttering speakers. Next, we compare our VBM findings with previous literature. Third, we focus our discussions on our findings regarding the connectivities involving the BGTC (see Fig. 1). We will use these altered connectivities to explain the findings about the activation patterns. Finally, we will mention the limitations of this study and draw conclusions.

4.1. Activation patterns

Previous research has found that, compared to non-stuttering speakers, stuttering speakers show greater activation in the right frontal operculum (FO)/anterior insula and cerebellum

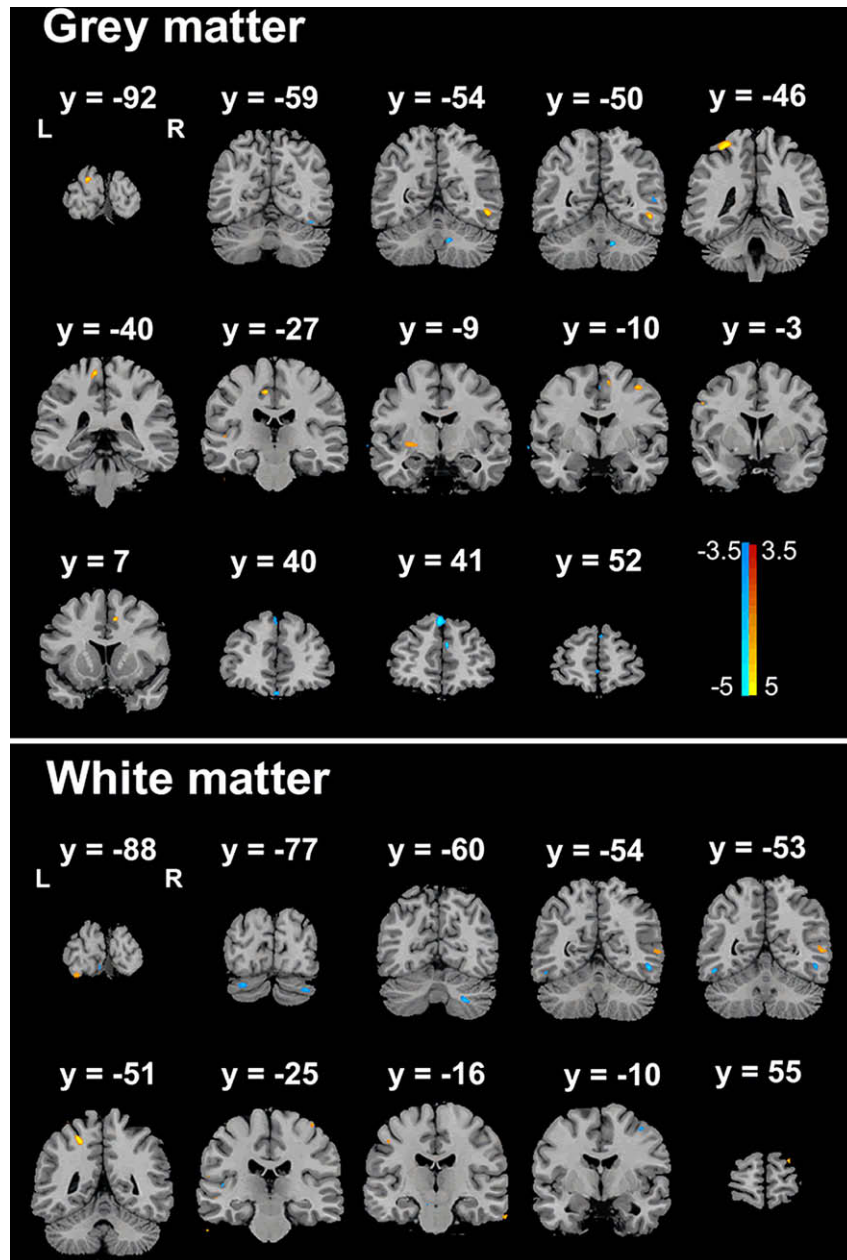


Fig. 5 – Regions that showed significant differences in GM (up) and WM (bottom) volume concentration between stuttering and non-stuttering speakers. Warm blobs indicate greater volume concentration in stuttering speakers than that of non-stuttering speakers, and cold blobs indicate less volume concentration in stuttering speakers than that of non-stuttering speakers. $p < .05$ (corrected).

(Brown et al., 2005). The present study replicated both of these so-called neural signatures of stuttering. Specifically, we found that stuttering speakers demonstrated greater activations in the right inferior frontal gyrus (BA44/46) and anterior insula (BA13) and cerebellum than did non-stuttering speakers. We also confirmed the overactivations in the bilateral sensorimotor and medial frontal motor areas (BA1/2/6) and the superior and middle frontal areas (BA9) among stuttering speakers (Braun et al., 1997; Brown et al., 2005; De Nil et al., 2008; Neumann et al., 2003). Previous research shows that the middle frontal gyrus, inferior frontal gyrus, and anterior insula are involved in phonological

representations (Bles and Jansma, 2008; Tan et al., 2005), whereas the medial and lateral motor areas are involved in the sequence control of speech movement (Alario et al., 2006). Therefore, the activation differences in these frontal regions strongly suggest that stuttering is associated with the dysfunction of phonological representation and movement control.

The third neural signature of stuttering is the under-activation in the bilateral anterior temporal cortex, which was only partially replicated by our results. Similar to Watkins et al. (2008), we found such under-activation only in the left ASTG (BA38), but not in the right temporal cortex. At the

Table 5 – Brain areas that showed increased and decreased grey and WM volume concentration in stuttering speakers as compared with non-stuttering controls.

| Brain area | x | y | z | z-Value | Volume |
|---|-----|-----|-----|---------|--------|
| GM | | | | | |
| Stuttering speakers > non-stuttering speakers | | | | | |
| R_Medial Frontal Gyrus (BA32) | 7 | 7 | 44 | 3.74 | 60 |
| R_Medial Frontal Gyrus (BA6) ^a | 8 | -10 | 56 | 3.47 | 37 |
| L_Precentral Gyrus (BA6) ^a | -50 | -3 | 36 | 3.34 | 23 |
| R_Precentral Gyrus (BA6) | 34 | -10 | 51 | 3.79 | 142 |
| L_Superior Parietal Lobule (BA7) | -32 | -46 | 56 | 4.06 | 541 |
| L_Paracentral Lobule (BA5) | -11 | -40 | 60 | 3.84 | 191 |
| R_Fusiform Gyrus (BA37) | 44 | -54 | -7 | 3.90 | 223 |
| L_Middle Occipital Gyrus (BA18) | -14 | -92 | 12 | 3.80 | 139 |
| L_Cingulate Gyrus (BA31) | -9 | -27 | 45 | 3.90 | 86 |
| R_Cingulate Gyrus (BA23) | 7 | -18 | 32 | 3.43 | 54 |
| L_Putamen | -29 | -9 | 0 | 3.42 | 212 |
| Non-stuttering speakers > Stuttering speakers | | | | | |
| L_Superior Frontal Gyrus (BA8) | -2 | 38 | 49 | 4.04 | 468 |
| L_Medial Frontal Gyrus (BA10) | -1 | 52 | 6 | 3.28 | 58 |
| L_Medial Frontal Gyrus (BA11) | -1 | 40 | -14 | 3.45 | 122 |
| R_Medial Frontal Gyrus (BA9) | 4 | 40 | 29 | 4.12 | 255 |
| L_Superior Temporal Gyrus (BA21) | -65 | -6 | -1 | 3.60 | 86 |
| R_Middle Temporal Gyrus (BA39) | 47 | -54 | 7 | 3.31 | 52 |
| R_Cerebellar Tonsil | 10 | -50 | -32 | 3.71 | 135 |
| R_Declive | 34 | -59 | -16 | 3.56 | 45 |
| R_Culmen of Vermis | 3 | -63 | -5 | 3.35 | 49 |
| WM | | | | | |
| Stuttering speakers > non-stuttering speakers | | | | | |
| R_Superior Frontal Gyrus (BA9) | 22 | 55 | 32 | 4.04 | 119 |
| L_Precuneus (BA7) | -22 | -51 | 45 | 5.24 | 832 |
| R_Inferior Temporal Gyrus (BA20) | 62 | -16 | -22 | 4.20 | 60 |
| R_Middle Temporal Gyrus (BA39) | 50 | -54 | 5 | 4.09 | 270 |
| L_Declive | -24 | -88 | -21 | 4.02 | 101 |
| Non-stuttering speakers > Stuttering speakers | | | | | |
| R_Precentral Gyrus (BA6) ^a | 34 | -10 | 53 | 3.99 | 34 |
| L_Superior Temporal Gyrus (BA41) ^a | -44 | -25 | 8 | 3.95 | 27 |
| L_Fusiform Gyrus (BA37) | -46 | -52 | -14 | 4.16 | 73 |
| R_Fusiform Gyrus (BA37) | 45 | -54 | -9 | 4.47 | 224 |
| L_Lingual Gyrus (BA18) | -4 | -87 | -15 | 4.15 | 99 |
| L_Tuber | -27 | -76 | -29 | 4.32 | 373 |
| R_Cerebellar Tonsil | 24 | -60 | -39 | 4.33 | 186 |
| R_Pyramis | 31 | -77 | -31 | 4.18 | 472 |

Note: $p < .05$, corrected for multiple comparisons. The coordinates were in LPI orientation of standard Talairach Space. Areas were sorted according to the anatomical lobe.

^a Areas did not survive the threshold.

same time, we additionally revealed greater activations in the posterior temporal cortex in stuttering speakers than in non-stuttering speakers. It is especially worth noting that the differential activation patterns we found for the anterior and posterior temporal cortex are consistent with previous results. De Nil et al. (2008) reported that non-stuttering speakers showed peak activation in the left superior temporal gyrus ($y = 2$) during the overt speech task, but no such activation was present in the stuttering speakers. Brown et al.'s (2005) meta-analysis also pointed out that the location of absent activation in stuttering speakers is in the anterior part of the temporal cortex ($y \approx -3$). In addition, De Nil et al. (2008) reported hyper-activated posterior temporal cortex [including both the superior ($y = -36$) and middle temporal gyrus ($y = -22$)] among stuttering speakers as compared to non-stuttering controls. The present results confirmed both hypoactivity in the anterior temporal cortex and hyperactivity in the posterior temporal cortex. This finding is also in line with previous results from non-stuttering speakers showing that the anterior and posterior parts of the temporal cortex may play different roles in speech (e.g., Rauschecker and Tian, 2003; Scott et al., 2000; Specht and Reul, 2003).

In terms of the model we specified in the introduction, we found neural differences in all five selected brain regions. The findings in the preSMA and temporal cortex have been discussed above. The greater activation in the left putamen and less activation in the thalamus in stuttering speakers than in non-stuttering speakers are also consistent with previous findings (Braun et al., 1997; Ludlow and Loucks, 2003; Watkins et al., 2008). Although Brown et al.'s (2005) meta-analysis did not find difference in the putamen, the differences found in the SMA may be related to the dysfunction of the putamen. The putamen is a part of the basal ganglia that is especially relevant to motor control. Many researchers have suspected an abnormal communication between the basal ganglia and the cerebral cortex for stuttering speakers (Smits-Bandstra and De Nil, 2007; Watkins et al., 2008). We will further discuss this issue in the connectivity section.

4.2. Anatomical differences

4.2.1. WM differences

In our VBM results, WM differences between stuttering and non-stuttering speakers mainly showed increased volume concentration among stuttering speakers in the right frontal and temporal cortex. Jäncke et al. (2004) and Beal et al. (2007) also reported similar findings that stuttering adults demonstrated increased WM volume concentration in the right frontal cortex (including the anterior middle frontal gyrus, inferior frontal gyrus, and precentral gyrus) and temporal cortex (the superior temporal gyrus). In contrast, no such increases of volume concentration were found in stuttering children (Chang et al., 2008). Thus, these results suggest an increased intrahemispheric communication within these areas and a possible dysfunction in the left frontal and temporal cortex in stuttering speakers.

Stuttering speakers showed decreased volume concentration in the left superior temporal gyrus and lingual gyrus

and the bilateral fusiform gyri and cerebellum. In the right hemisphere, only the precentral gyrus demonstrated decreased volume concentration. Such results have not been reported previously (Beal et al., 2007; Jäncke et al., 2004). However, Sommer et al. (2002) and Watkins et al. (2008) found lower fractional anisotropy (FA) value in the left rolandic operculum (RO)/FO immediately above the Sylvian fissure in stuttering adults. Chang et al. (2008) found the same result in stuttering children. Considering the small sample size of the present study and the limitations of VBM methods, we might have failed to detect anatomical differences in this region. Importantly, the inferior arcuate fascicle immediately surrounds this region and links the temporal and frontal speech regions. It is possible that the WM volume differences underneath the RO/FO have influenced other connected regions such as the left temporal cortex and even the lingual gyrus. Recent studies showed that the cerebellum seems to be related to these speech regions by participating in the temporal organization of internal speech and subserving the online sequencing of syllables (Ackermann, 2008; Ackermann et al., 2007). Therefore, the decrease of volume concentration in the cerebellum may also be related to possible disconnections among the left speech regions.

4.2.2. GM differences

In the VBM results, stuttering speakers showed increased volume concentration in the bilateral precentral gyri, occipital-temporal regions, and cingulate gyrus. The changes in the medial frontal gyrus only appeared in the right hemisphere whereas the changes in the superior parietal lobule and paracentral gyrus only appeared in the left hemisphere. These widely distributed increases of GM volume concentration in stuttering adults have been reported in previous studies although the specific locations may be different (Beal et al., 2007; Cykowski et al., 2008; Foundas et al., 2001; but see Jäncke et al., 2004). No similar increases are evident in stuttering children (Chang et al., 2008). Recent research has showed that extensive practice of a behavior can increase the volume concentration (Draganski et al., 2004; Gaser and Schlaug, 2003). Thus, these GM changes may have resulted from persistent stuttering.

Decreased GM volume concentration in stuttering speakers was found mainly in the left side of the cerebral cortex (including the superior and medial frontal gyri, superior temporal gyrus) and the right side of the cerebellum. Previous studies rarely reported decreased GM volume concentration in stuttering adults (Beal et al., 2007; Jäncke et al., 2004). One of the few exceptions was Foundas et al. (2003, 2004) who reported reduced left/right asymmetries (suggesting decreased GM volume concentration) in the prefrontal and temporal cortex. Chang et al. (2008) also found decreased GM volume concentration in the left inferior frontal gyrus and bilateral temporal regions in stuttering children. Future research needs to replicate these results and examines developmental differences.

Of greater relevance to our SEM model, the present study revealed that the ASTG (BA21) showed a significant decrease of GM volume concentration whereas the left posterior

superior temporal gyrus (BA41) showed a decrease of WM volume concentration among the stuttering speakers. Moreover, the left putamen showed a significant increase of GM volume concentration among stuttering speakers. These results will be further discussed in a subsequent section about the SEM results. Taken together both sets of findings (those consistent with previous studies and those newly revealed in our study), we think a strong case can be made that the impairment of the BGTC plays a special role in stuttering.

4.3. Similarities and differences in effective connectivity

Activation patterns associated with stuttering may well be due to differences in effective connectivity. In this section, we will discuss the connections within the BGTC.

4.3.1. Connectivity between the basal ganglia-thalamus and preSMA

As specified in our model (see Fig. 1), the preSMA receives input from the thalamus, which in turn receives input from the basal ganglia. This connection is hypothesized to be important for syllable representation and serial coordination of motor apparatus (e.g., Alario et al., 2006; Crosson et al., 2001; Hikosaka et al., 1996) as well as for the selection, initiation, and inhibition of action and movement timing control (e.g., Cunnington et al., 2006; Jaffard et al., 2008). Our SEM results showed that stuttering speakers and non-stuttering speakers differed significantly in this connection: a strong negative projection in non-stuttering speakers, but a positive projection in stuttering speakers. One interpretation of this result is that the negative project for non-stuttering speakers indicates ordered timing and sequencing signals provided for the preSMA by the basal ganglia-thalamus, whereas the positive projection for stuttering speakers may indicate insufficient control signal and much unordered signal input from the basal ganglia-thalamus, thus resulting in uncontrolled hyperactivity in the preSMA (see Fig. 3). These results reflect stuttering speakers' difficulties (but not incapability) in the selection and sequencing of speech movements (e.g., Blomgren et al., 1998; Dworzynski et al., 2003; Howell and Au-Yeung, 1995; Melnick and Conture, 2000; Ning et al., 2007).

In terms of output of the preSMA, our results showed no significant differences between stuttering and non-stuttering speakers. For both stuttering and non-stuttering speakers, the preSMA provided a positive input to the putamen. This indicates that the role of the output from the preSMA to the basal ganglia-thalamus in speech may be different from that of the projection from the basal ganglia-thalamus to the preSMA. One brain infarction study (Exner et al., 2002) found that people with focal lesions restricted to the basal ganglia showed unimpaired motor sequence function, but had more difficulties improving their general proficiency for sequence execution. It has also been suggested that for action control, the SMA assembles the sequence of the action, whereas the basal ganglia update its parameters and store them (Gentilucci et al., 2000). Taken together, it appears that the output from the preSMA to the basal ganglia-thalamus provides specific associations between speech movements, which do

not seem to be impaired in stuttering speakers. In contrast, the projection from the basal ganglia-thalamus to the preSMA adjusts the latter's function as it receives convergent input from the entire cerebral cortex (Parent, 1996). This adjustment function seems to be impaired in stuttering speakers (Blomgren and Goberman, 2008; Namasivayam and van Lieshout, 2008; Smits-Bandstra and De Nil, 2007).

4.3.2. Connectivity between the basal ganglia-thalamus and the temporal cortex

In our model, we assumed a recursive connection between the basal ganglia-thalamus and the posterior temporal cortex. This connection is supported by the evidence that the basal ganglia-thalamus is anatomically connected with the temporal cortex (e.g., Behrens et al., 2003; Leh et al., 2007; Middleton and Strick, 1996). Moreover, functional connections also exist because the posterior temporal cortex as well as the SMA and basal ganglia have been found to be involved in auditory-motor representations and temporal sequence control of movement regardless of the modality (Karabanov et al., 2009; Kimura et al., 2008; Remy et al., 2008). The present SEM results showed a significantly stronger projection from the basal ganglia-thalamus to the PMTG in stuttering speakers than in non-stuttering speakers. In addition, there was a negative input from the PMTG to the basal ganglia-thalamus in non-stuttering speakers, but not in stuttering speakers. These results suggest that although there is a strong projection to the PMTG in stuttering speakers, the PMTG may be unable to receive the required timing control signals from the basal ganglia-thalamus, thus exhibiting hyper-activation (see Fig. 3). One possible explanation is that the lack of input from the PMTG to the basal ganglia-thalamus in stuttering speakers makes it impossible for the basal ganglia-thalamus to provide such control signals. However, considering that the basal ganglia-thalamus do not solely depend on the PMTG to generate control signals and there are normal input from the preSMA and the anterior temporal cortex, the most reasonable explanation is that the projection from the basal ganglia-thalamus to the PMTG is impaired, which results in the PMTG's failure to retrieve phonological codes during speech (Bles and Jansma, 2008; Indefrey and Levelt, 2004).

For the connection from the anterior temporal cortex to the basal ganglia-thalamus, both stuttering and non-stuttering speakers had a positive input and did not show significant group differences. This input as well as the inputs from the preSMA and the posterior temporal cortex are assumed to be converged in the basal ganglia-thalamus and mediated by the globus pallidus and substantia nigra. They end up in different parts of the thalamus, and then project to the cerebral cortex to provide internal timing cues to facilitate the selection and initiation of appropriate output while inhibiting unwanted output in a well-learned sequence (e.g., Cunnington et al., 1996; McFarland and Haber, 2002; van der Graaf et al., 2004). The absence of group differences in this connection suggests that, like the function of the preSMA, the auditory feedback function of the anterior temporal cortex in stuttering speakers seems to be intact. Its under-activity may have resulted from interactions with other regions.

4.3.3. Connectivity from the posterior to the anterior temporal cortex

Our model also included a connection from the posterior temporal cortex to the anterior temporal cortex. Previous research has indicated a strong functional connectivity between the anterior and posterior perisylvian language areas (Hickok and Poeppel, 2004; Horwitz and Braun, 2004). The projection from the posterior temporal cortex to the anterior temporal cortex may reflect the efference copy of the speech movement plan. According to the efference copy theory (Gallistel, 1980), when a motor command is sent through the nervous system, a copy of the motor plan is projected to the perceptual regions and used to predict the expected sensation that will occur. Brown et al. (2005) used the efference copy theory to explain the under-activated temporal cortex. For example, the authors proposed that the perceptual prediction of speech sounds is being delivered repeatedly to the auditory system as an inhibitory signal that will attenuate the effects of any successful utterances, and will further result in under-activity in the auditory areas. However, their under-activated auditory area was located in the more anterior part of the temporal cortex ($y \approx -3$), while the dampened auditory areas in the literature about non-stuttering speakers were more posterior (Curio et al., 2000; Houde et al., 2002).

In addition, recent interpretations about the efference copy have described these projections not as uniquely inhibitory, but also inclusive of any transient modulatory input (Poulet and Hedwig, 2007). Based on our assumption in the SEM model and our results, we propose a different explanation. Our SEM results showed a strong negative projection in the stuttering speakers, but a positive projection in non-stuttering speakers. This difference may reflect an out-of-order timing control of speech movement issued from the posterior temporal cortex and from the basal ganglia-thalamus. The efference copy of this out-of-order motor control signal may fail to modulate the auditory feedback function, resulting in less activation in the anterior temporal cortex in stuttering speakers than in non-stuttering speakers. Watkins et al. (2008) reached a similar conclusion that the under-activity in the anterior temporal cortex of stuttering speakers may reflect reduced inputs from the motor system during speech production. In non-stuttering speakers, since the issued motor plan is intact, its efference copy is not necessarily to be inhibition but rather facilitation so as to increase the auditory feedback function. In summary, the present results suggested an influence of impaired timing control in the motor plan, not the efference copy, on the under-activity of the anterior temporal cortex.

4.3.4. Connectivity from the anterior and posterior temporal cortex to the preSMA

Considering the integrative function of the temporal cortex and the frontal cortex, an output from the anterior and posterior temporal cortex to the preSMA was specified in the BGTC model (Hagmann et al., 2008). For the output from the posterior temporal cortex to the preSMA, no significant differences between stuttering and non-stuttering speakers were found. Considering the involvement in inhibition control

of both the preSMA and the posterior temporal cortex (Allen et al., 2008; Nakata et al., 2008), this connection may constitute a sub-circuit of auditory-motor representation (Hickok and Poeppel, 2004), which seems to be intact in stuttering speakers.

The output from the anterior temporal cortex to the preSMA is assumed to have a role in directly modulating the function of the frontal motor cortex through auditory feedback (Christoffels et al., 2007). In the present study, we found that stuttering speakers had a stronger output than did non-stuttering speakers. As both stuttering and non-stuttering speakers had a positive input to the basal ganglia-thalamus (see above), the auditory feedback function of the anterior temporal cortex was not impaired. The difference in the output to the preSMA between stuttering and non-stuttering speakers was likely due to external influence, i.e., the projection from the posterior temporal cortex. This result suggests that, although auditory feedback dysfunction is not the cause of stuttering, it may have influence on the severity of stuttering.

4.3.5. Connectivity from the basal ganglia to the thalamus

The dysfunction in the medial frontal cortex and the posterior temporal cortex both point to a potential impairment of the basal ganglia-thalamus in stuttering speakers. In the present results, stuttering speakers showed a stronger projection from the putamen to the thalamus than did non-stuttering speakers. This result makes sense because the basal ganglia have been found to correlate positively to the stuttering rate (in the case of the putamen) (Braun et al., 1997) and stuttering severity (in the case of the caudate nucleus) (Giraud et al., 2008). Further, the correlation disappeared when stuttering is improved (Giraud et al., 2008). Brain lesion data suggest that the occurrence of and recovery from stuttering are associated, respectively, with damages and recovery in the basal ganglia-thalamus (Kent, 2000; Ludlow and Loucks, 2003). As Alm (2004) argued, the basal ganglia-thalamus may play an especially important role in the possible focal disturbance of stuttering. However, almost all of the previous results about the basal ganglia-thalamus are related to the motor areas. Few studies have discussed their relation with the temporal areas. The results of the present study suggest that the potential impairment of the basal ganglia-thalamus may be related to the dysfunctions of both the frontal motor cortex and the temporal auditory cortex.

4.4. Relations between altered connectivity and anatomical structural changes

The above reasoning about the altered effective connectivity seems to point to a focal impairment of the basal ganglia-thalamus, that is, their failure to provide the timing control signals. However, the VBM results revealed a significant increase of GM volume concentration in the left putamen. Previous research has showed that the GM volume concentration will increase with continuous training or practicing (Draganski et al., 2004; Gaser and Schlaug, 2003). Thus, the basal ganglia-thalamus of stuttering speakers seems to work well in delivering the output signal, but may experience difficulties in projecting the output signals to the cerebral

cortex. The repeated attempt to project may lead to increases in both the GM volume and activation in the putamen.

The VBM results further revealed a decrease of GM volume concentration in the anterior temporal cortex and the anterior medial frontal cortex. At the same time, a decrease of WM volume concentration was found in the region underlying the posterior temporal cortex. These results seem to indicate impairment related to the projection from the basal ganglia-thalamus to the cerebral cortex as brain lesions studies have showed a tendency toward smaller regional volumes in the left preSMA of subjects with basal ganglia lesions (Exner et al., 2002). Although regions in the left medial frontal gyrus showing GM decrease do not overlap with the selected region of the preSMA, they are closely related to the preSMA (Cunnington et al., 2006; Geyer, 2004; Jaffard et al., 2008). Taken together, the altered connectivity and the anatomical structural changes in the BGTC suggested an impairment of functional connection between the subcortical and cortical areas, which interrupts the timing control of speech.

The above conclusion is also consistent with previous findings. For example, in Watkins et al. (2008) study, both the over-activity in the substantia nigra and the under-activity in the motor areas were reported. They also suggested an important role of the cortico-striatal-thalamic loop in stuttering. The difference between Watkins et al.'s (2008) study and the present study was that they placed more emphasis on the WM abnormalities underlying the functional differences in ventral premotor cortex, whereas the present study emphasized the connection from the basal ganglia-thalamus to the cerebral cortex (including both the frontal motor and temporal auditory areas). However, both studies reached a similar conclusion that these abnormalities may interrupt the selection, initiation, and execution of motor sequences necessary for fluent speech production.

4.5. Limitations

Several limitations of the present study should be acknowledged. First, because SEM puts a limit on model complexity, not all of the brain regions, or all of the interconnections between brain regions, could be modeled in a single study. For example, the premotor/primary motor areas and cerebellum may be also important in stuttering but they were not included in the SEM model. Second, the functional connectivity between two brain areas does not necessarily reflect the anatomical connectivity between two areas because their functional coupling can be mediated by other areas not included in the model. The connection of the temporal language areas with the frontal language areas through the inferior arcuate fascicle is a good example to illustrate the present SEM model's limitation (Büchel and Sommer, 2004). Third, the present study examined functional connectivity only in the left hemisphere. Although previous literature suggests that stuttering is most likely due to dysfunctions in the left hemisphere, it is certainly worthwhile to include the right hemisphere in future analysis of larger and more extensive datasets. Fourth, the VBM method has its inherent limitations. For example, it does not take in account the issue of anisotropy and fiber crossing. Future research should also include other methods such as DTI. Fifth, the present study

used a block design, and consequently had poor temporal resolution. Future fMRI studies employing a rapid event-related design with a short TR, or EEG/ERP (event-related potential) or MEG studies may be helpful in elucidating the timing question. Finally, the small sample size of females did not allow us to examine sex differences in activity between male and female stuttering speakers (Ingham et al., 2004). Future studies with a larger dataset may contribute further information on this question.

5. Conclusion

By employing the multivariate technique of SEM, the present study revealed significant differences in effective connectivity among the nodes of the BGTC between stuttering speakers and non-stuttering controls. The connectivity differences included not only the subcortical–cortical interactions between the basal ganglia–thalamus and the frontal motor cortex (preSMA)/the temporal cortex (PMTG), but also interactions within the subcortical circuit from the putamen to the thalamus and the cerebral circuit from the PMTG to the ASTG and then to the preSMA. These results suggest connective disturbance between the basal ganglia–thalamus and the cerebral cortex (including both the frontal motor cortex and temporal auditory cortex), which affects the preSMA and posterior temporal cortex and thus disrupts the timing control in speech production. These conclusions were supported by the VBM results showing significant decreases of GM and WM volume concentration in the left superior and medial frontal gyri, superior temporal gyrus, and the right side of the cerebellum. Taken together the SEM and the VBM results, a strong conclusion can be drawn that developmental stuttering is a result of impaired communications among a widely distributed neural network in the left hemisphere, involving especially the basal ganglia–thalamus and the cerebral cortex within the BGTC. Connectivity impairments in this network and associated neural abnormalities constitute the neural signatures of developmental stuttering.

Acknowledgements

This work was supported by the Beijing Natural Science Foundation (7062037) and the National Pandeng Project (95-special-09) of China.

REFERENCES

Abe K, Yokoyama R, and Yorifuji S. Repetitive speech disorder resulting from infarcts in the paramedian thalamic and midbrain. *Journal of Neurology, Neurosurgery and Psychiatry*, 56: 1024–1026, 1993.

Ackermann H. Cerebellar contributions to speech production and speech perception: psycholinguistic and neurobiological perspectives. *Trends in Neurosciences*, 31: 265–272, 2008.

Ackermann H, Mathiak K, and Riecker A. The contribution of the cerebellum to speech production and speech perception: clinical and functional imaging data. *The Cerebellum*, 6: 202–213, 2007.

Alario FX, Chainay H, Lehericy S, and Cohen L. The role of the supplementary motor area (SMA) in word production. *Brain Research*, 1076: 129–143, 2006.

Alexander GE, DeLong MR, and Strick PL. Parallel organization of functionally segregated circuits linking basal ganglia and cortex. *Annual Review of Neuroscience*, 9: 357–381, 1986.

Allen P, Mechelli A, Stephan KE, Day F, Dalton J, Williams S, et al. Fronto-temporal interactions during overt verbal initiation and suppression. *Journal of Cognitive Neuroscience*, 20: 1656–1669, 2008.

Alm PA. Stuttering and the basal ganglia circuits: a critical review of possible relations. *Journal of Communication Disorders*, 37: 325–369, 2004.

Andrews G, Craig A, Feyer AM, Hoddinott S, Howie P, and Neilson M. Stuttering: a review of research findings and theories circa 1982. *Journal of Speech and Hearing Disorders*, 48: 226–246, 1983.

Ashburner J and Friston KJ. Unified segmentation. *NeuroImage*, 26: 839–851, 2005.

Au Duong MV, Boulanouar K, Audoin B, Treseras S, Ibarrola D, Malikova I, et al. Modulation of effective connectivity inside the working memory network in patients at the earliest stage of multiple sclerosis. *NeuroImage*, 24: 533–538, 2005.

Büchel C, Coull JT, and Friston KJ. The predictive value of changes in effective connectivity for human learning. *Science*, 283: 1538–1541, 1999.

Büchel C and Friston KJ. Modulation of connectivity in visual pathways by attention: cortical interactions evaluated with structural equation modelling and fMRI. *Cerebral Cortex*, 7: 768–778, 1997.

Büchel C and Sommer M. What causes stuttering? *PLoS Biology*, 2: E46, 2004.

Beal DS, Gracco VL, Lafaille SJ, and De Nil LF. Voxel-based morphometry of auditory and speech-related cortex in stutterers. *Neuroreport*, 18: 1257–1260, 2007.

Behrens TE, Johansen-Berg H, Woolrich MW, Smith SM, Wheeler-Kingshott CA, Boulby PA, et al. Non-invasive mapping of connections between human thalamus and cortex using diffusion imaging. *Nature Neuroscience*, 6: 750–757, 2003.

Bentler PM. Comparative fit indexes in structural models. *Psychological Bulletin*, 107: 238–246, 1990.

Bles M and Jansma BM. Phonological processing of ignored distractor pictures, an fMRI investigation. *BMC Neuroscience*, 9: 20, 2008.

Blomgren M and Goberman AM. Revisiting speech rate and utterance length manipulations in stuttering speakers. *Journal of Communication Disorders*, 41: 159–178, 2008.

Blomgren M, Robb M, and Chen Y. A note on vowel centralization in stuttering and nonstuttering individuals. *Journal of Speech, Language, and Hearing Research*, 41: 1042–1051, 1998.

Boberg E, Yeudall L, Schopflocher D, and Bo-Lassen P. The effect of an intensive behavioral program on the distribution of EEG alpha power in stutterers during the processing of verbal and visuospatial information. *Journal of Fluency Disorders*, 8: 245–263, 1983.

Bohland JW and Guenther FH. An fMRI investigation of syllable sequence production. *NeuroImage*, 32: 821–841, 2006.

Braun AR, Varga M, Stager S, Schulz G, Selbie S, Maisog JM, et al. Altered patterns of cerebral activity during speech and language production in developmental stuttering. An h2(15)o positron emission tomography study. *Brain*, 120: 761–784, 1997.

Brodal P. *The Central Nervous System: Structure and Function*. USA: Oxford University Press, 2004.

Brown S, Ingham RJ, Ingham JC, Laird AR, and Fox PT. Stuttered and fluent speech production: an ale meta-analysis of functional neuroimaging studies. *Human Brain Mapping*, 25: 105–117, 2005.

- Browne MW and Cudeck R. Alternative ways of assessing model fit. In Bollen KA and Long JS (Eds), *Testing Structural Equation Models*. Newbury Park: Sage Publications, 1993: 136–162.
- Bullmore E, Horwitz B, Honey G, Brammer M, Williams S, and Sharma T. How good is good enough in path analysis of fMRI data? *NeuroImage*, 11: 289–301, 2000.
- Chang SE, Erickson KI, Ambrose NG, Hasegawa-Johnson MA, and Ludlow CL. Brain anatomy differences in childhood stuttering. *NeuroImage*, 39: 1333–1344, 2008.
- Christoffels IK, Formisano E, and Schiller NO. Neural correlates of verbal feedback processing: an fMRI study employing overt speech. *Human Brain Mapping*, 28: 868–879, 2007.
- Cox RW. AFNI: software for analysis and visualization of functional magnetic resonance neuroimages. *Computers and Biomedical Research*, 29: 162–173, 1996.
- Cox RW and Jesmanowicz A. Real-time 3D image registration for functional MRI. *Magnetic Resonance in Medicine*, 42: 1014–1018, 1999.
- Craig A and Tran Y. The epidemiology of stuttering: the need for reliable estimates of prevalence and anxiety levels over the lifespan. *International Journal of Speech-Language Pathology*, 7: 41–46, 2005.
- Crosson B, Sadek JR, Maron L, Gokcay D, Mohr CM, Auerbach EJ, et al. Relative shift in activity from medial to lateral frontal cortex during internally versus externally guided word generation. *Journal of Cognitive Neuroscience*, 13: 272–283, 2001.
- Cunnington R, Bradshaw JL, and Iansek R. The role of the supplementary motor area in the control of voluntary movement. *Human Movement Science*, 15: 627–647, 1996.
- Cunnington R, Windischberger C, Robinson S, and Moser E. The selection of intended actions and the observation of others' actions: a time-resolved fMRI study. *NeuroImage*, 29: 1294–1302, 2006.
- Curio G, Neuloh G, Numminen J, Jousmaki V, and Hari R. Speaking modifies voice-evoked activity in the human auditory cortex. *Human Brain Mapping*, 9: 183–191, 2000.
- Curry FK and Gregory HH. The performance of stutterers on dichotic listening tasks thought to reflect cerebral dominance. *Journal of Speech and Hearing Research*, 12: 73–82, 1969.
- Cykowski MD, Kochunov PV, Ingham RJ, Ingham JC, Mangin JF, Riviere D, et al. Perisylvian sulcal morphology and cerebral asymmetry patterns in adults who stutter. *Cerebral Cortex*, 18: 571–583, 2008.
- De Nil LF, Beal DS, Lafaille SJ, Kroll RM, Crawley AP, and Gracco VL. The effects of simulated stuttering and prolonged speech on the neural activation patterns of stuttering and nonstuttering adults. *Brain and Language*, 107: 114–123, 2008.
- De Nil LF, Kroll RM, Kapur S, and Houle S. A positron emission tomography study of silent and oral single word reading in stuttering and nonstuttering adults. *Journal of Speech, Language, and Hearing Research*, 43: 1038–1053, 2000.
- De Nil LF, Kroll RM, Lafaille SJ, and Houle S. A positron emission tomography study of short- and long-term treatment effects on functional brain activation in adults who stutter. *Journal of Fluency Disorders*, 28: 357–379. quiz 379–380, 2003.
- Della-Maggiore V, Sekuler AB, Grady CL, Bennett PJ, Sekuler R, and McIntosh AR. Corticolumbic interactions associated with performance on a short-term memory task are modified by age. *Journal of Neuroscience*, 20: 8410–8416, 2000.
- Doeller CF, Opitz B, Krick CM, Mecklinger A, and Reith W. Differential hippocampal and prefrontal–striatal contributions to instance-based and rule-based learning. *NeuroImage*, 31: 1802–1816, 2006.
- Draganski B, Gaser C, Busch V, Schuierer G, Bogdahn U, and May A. Neuroplasticity: changes in grey matter induced by training. *Nature*, 427: 311–312, 2004.
- Dworzynski K, Howell P, and Natke U. Predicting stuttering from linguistic factors for German speakers in two age groups. *Journal of Fluency Disorders*, 28: 95–112. quiz 112–113, 2003.
- Everbusch O, Nadoleczny M, Howe L, Francis LM, and McCord CP. *Diseases of the Eye and Disorders of Speech in Childhood*. London: J. B. Lippincott, 1914.
- Exner C, Koschack J, and Irle E. The differential role of premotor frontal cortex and basal ganglia in motor sequence learning: evidence from focal basal ganglia lesions. *Learning and Memory*, 9: 376–386, 2002.
- Ferrandez AM, Hugueville L, Lehericy S, Poline JB, Marsault C, and Pouthas V. Basal ganglia and supplementary motor area subvent duration perception: an fMRI study. *NeuroImage*, 19: 1532–1544, 2003.
- Fletcher P, McKenna PJ, Friston KJ, Frith CD, and Dolan RJ. Abnormal cingulate modulation of fronto-temporal connectivity in schizophrenia. *NeuroImage*, 9: 337–342, 1999.
- Forman SD, Cohen JD, Fitzgerald M, Eddy WF, Mintun MA, and Noll DC. Improved assessment of significant activation in functional magnetic resonance imaging (fMRI): use of a cluster-size threshold. *Magnetic Resonance in Medicine*, 33: 636–647, 1995.
- Foundas AL, Bollich AM, Corey DM, Hurley M, and Heilman KM. Anomalous anatomy of speech-language areas in adults with persistent developmental stuttering. *Neurology*, 57: 207–215, 2001.
- Foundas AL, Bollich AM, Feldman J, Corey DM, Hurley M, Lemen LC, et al. Aberrant auditory processing and atypical planum temporale in developmental stuttering. *Neurology*, 63: 1640–1646, 2004.
- Foundas AL, Corey DM, Angeles V, Bollich AM, Crabtree-Hartman E, and Heilman KM. Atypical cerebral laterality in adults with persistent developmental stuttering. *Neurology*, 61: 1378–1385, 2003.
- Fox PT, Ingham RJ, Ingham JC, Hirsch TB, Downs JH, Martin C, et al. A pet study of the neural systems of stuttering. *Nature*, 382: 158–161, 1996.
- Fox PT, Ingham RJ, Ingham JC, Zamarripa F, Xiong JH, and Lancaster JL. Brain correlates of stuttering and syllable production. A pet performance-correlation analysis. *Brain*, 123: 1985–2004, 2000.
- Friston KJ, Harrison L, and Penny W. Dynamic causal modelling. *NeuroImage*, 19: 1273–1302, 2003.
- Fu CH, McIntosh AR, Kim J, Chau W, Bullmore ET, Williams SC, et al. Modulation of effective connectivity by cognitive demand in phonological verbal fluency. *NeuroImage*, 30: 266–271, 2006.
- Gallistel CR. *The Organization of Action: a New Synthesis*. Hillsdale: Lawrence Erlbaum Associates, 1980.
- Gaser C and Schlaug G. Gray matter differences between musicians and nonmusicians. *Annals of the New York Academy of Sciences*, 999: 514–517, 2003.
- Gentilucci M, Bertolani L, Benuzzi F, Negrotti A, Pavesi G, and Gangitano M. Impaired control of an action after supplementary motor area lesion: a case study. *Neuropsychologia*, 38: 1398–1404, 2000.
- Geyer S. The microstructural border between the motor and the cognitive domain in the human cerebral cortex. *Advances in Anatomy, Embryology and Cell Biology*, 174: 1–89, 2004.
- Giraud AL, Neumann K, Bachoud-Levi AC, von Gudenberg AW, Euler HA, Lanfermann H, et al. Severity of dysfluency correlates with basal ganglia activity in persistent developmental stuttering. *Brain and Language*, 104: 190–199, 2008.
- Goncalves MS, Hall DA, Johnsrude IS, and Haggard MP. Can meaningful effective connectivities be obtained between auditory cortical regions? *NeuroImage*, 14: 1353–1360, 2001.

- Good CD, Johnsrude IS, Ashburner J, Henson RN, Friston KJ, and Frackowiak RS. A voxel-based morphometric study of ageing in 465 normal adult human brains. *NeuroImage*, 14: 21–36, 2001.
- Hagmann P, Cammoun L, Gigandet X, Meuli R, Honey CJ, Wedeen VJ, et al. Mapping the structural core of human cerebral cortex. *PLoS Biology*, 6: e159, 2008.
- Hickok G and Poeppel D. Dorsal and ventral streams: a framework for understanding aspects of the functional anatomy of language. *Cognition*, 92: 67–99, 2004.
- Higham NJ. Optimization by direct search in matrix computations. *SIAM Journal on Matrix Analysis and Applications*, 14: 317–333, 1993.
- Hikosaka O, Sakai K, Miyauchi S, Takino R, Sasaki Y, and Putz B. Activation of human presupplementary motor area in learning of sequential procedures: a functional MRI study. *Journal of Neurophysiology*, 76: 617–621, 1996.
- Honey GD, Suckling J, Zelaya F, Long C, Routledge C, Jackson S, et al. Dopaminergic drug effects on physiological connectivity in a human cortico-striato-thalamic system. *Brain*, 126: 1767–1781, 2003.
- Horwitz B and Braun AR. Brain network interactions in auditory, visual and linguistic processing. *Brain and Language*, 89: 377–384, 2004.
- Houde JF, Nagarajan SS, Sekihara K, and Merzenich MM. Modulation of the auditory cortex during speech: an MEG study. *Journal of Cognitive Neuroscience*, 14: 1125–1138, 2002.
- Howell P and Au-Yeung J. The association between stuttering, brown's factors, and phonological categories in child stutterers reading in age between 2 and 12 years. *Journal of Fluency Disorders*, 20: 331–344, 1995.
- Iidaka T, Matsumoto A, Nogawa J, Yamamoto Y, and Sadato N. Frontoparietal network involved in successful retrieval from episodic memory. Spatial and temporal analyses using fMRI and ERP. *Cerebral Cortex*, 16: 1349–1360, 2006.
- Indefrey P and Levelt WJ. The spatial and temporal signatures of word production components. *Cognition*, 92: 101–144, 2004.
- Ingham RJ, Fox PT, Costello Ingham J, and Zamarripa F. Is overt stuttered speech a prerequisite for the neural activations associated with chronic developmental stuttering? *Brain and Language*, 75: 163–194, 2000.
- Ingham RJ, Fox PT, Ingham JC, Xiong J, Zamarripa F, Hardies LJ, et al. Brain correlates of stuttering and syllable production: gender comparison and replication. *Journal of Speech, Language, and Hearing Research*, 47: 321–341, 2004.
- Ingham RJ, Ingham JC, Finn P, and Fox PT. Towards a functional neural systems model of developmental stuttering. *Journal of Fluency Disorders*, 28: 297–317. quiz 317–318, 2003.
- Jäncke L, Hanggi J, and Steinmetz H. Morphological brain differences between adult stutterers and non-stutterers. *BMC Neurology*, 4: 23, 2004.
- Jöreskog KG. Some contributions to maximum likelihood factor analysis. *Psychometrika*, 32: 443–482, 1967.
- Jöreskog KG and Sorbom D. *Lisrel 8. User's Reference Guide*. Chicago: Scientific Software International, 1996.
- Jaffard M, Longcamp M, Velay JL, Anton JL, Roth M, Nazarian B, et al. Proactive inhibitory control of movement assessed by event-related fMRI. *NeuroImage*, 42: 1196–1206, 2008.
- Karabanov A, Blom O, Forsman L, and Ullen F. The dorsal auditory pathway is involved in performance of both visual and auditory rhythms. *NeuroImage*, 44: 480–488, 2009.
- Kent RD. Research on speech motor control and its disorders: a review and prospective. *Journal of Communication Disorders*, 33: 391–427. quiz 428, 2000.
- Kim J, Zhu W, Chang L, Bentler PM, and Ernst T. Unified structural equation modeling approach for the analysis of multisubject, multivariate functional MRI data. *Human Brain Mapping*, 28: 85–93, 2007.
- Kimura N, Kumamoto T, Hanaoka T, Hazama Y, Nakamura K, and Arakawa R. Corticobasal degeneration presenting with progressive conduction aphasia. *Journal of the Neurological Sciences*, 269: 163–168, 2008.
- Kolomiets BP, Deniau JM, Glowinski J, and Thierry AM. Basal ganglia and processing of cortical information: functional interactions between trans-striatal and trans-subthalamic circuits in the substantia nigra pars reticulata. *Neuroscience*, 117: 931–938, 2003.
- Leh SE, Ptito A, Chakravarty MM, and Strafella AP. Fronto-striatal connections in the human brain: a probabilistic diffusion tractography study. *Neuroscience Letters*, 419: 113–118, 2007.
- Lewis PA, Wing AM, Pope PA, Praamstra P, and Miall RC. Brain activity correlates differentially with increasing temporal complexity of rhythms during initialisation, synchronisation, and continuation phases of paced finger tapping. *Neuropsychologia*, 42: 1301–1312, 2004.
- Liu L, Peng D, Ding G, Jin Z, Zhang L, Li K, et al. Dissociation in the neural basis underlying Chinese tone and vowel production. *NeuroImage*, 29: 515–523, 2006.
- Lubke GH and Dolan CV. Can unequal residual variances across groups mask differences in residual means in the common factor model? *Structural Equation Modeling*, 10: 175–192, 2003.
- Ludlow CL and Loucks T. Stuttering: a dynamic motor control disorder. *Journal of Fluency Disorders*, 28: 273–295. quiz 295, 2003.
- McFarland NR and Haber SN. Thalamic relay nuclei of the basal ganglia form both reciprocal and nonreciprocal cortical connections, linking multiple frontal cortical areas. *Journal of Neuroscience*, 22: 8117–8132, 2002.
- McIntosh AR. Mapping cognition to the brain through neural interactions. *Memory*, 7: 523–548, 1999.
- McIntosh AR and Gonzalez-Lima F. Structural equation modeling and its application to network analysis in functional brain imaging. *Human Brain Mapping*, 2: 2–22, 1994a.
- McIntosh AR and Gonzalez-Lima F. Network interactions among limbic cortices, basal forebrain, and cerebellum differentiate a tone conditioned as a pavlovian excitator or inhibitor: fluorodeoxyglucose mapping and covariance structural modeling. *Journal of Neurophysiology*, 72: 1717–1733, 1994b.
- McIntosh AR, Grady CL, Ungerleider LG, Haxby JV, Rapoport SI, and Horwitz B. Network analysis of cortical visual pathways mapped with pet. *Journal of Neuroscience*, 14: 655–666, 1994.
- Melnick KS and Conture KG. Relationship of length and grammatical complexity to the systematic and nonsystematic speech errors and stuttering of children who stutter. *Journal of Fluency Disorders*, 25: 21–45, 2000.
- Middleton FA and Strick PL. The temporal lobe is a target of output from the basal ganglia. *Proceedings of the National Academy of Sciences of the United States of America*, 93: 8683–8687, 1996.
- Moore W. Hemispheric alpha asymmetries of stutterers and nonstutterers for the recall and recognition of words and connected reading passages: some relationships to severity of stuttering. *Journal of Fluency Disorders*, 11: 71–89, 1986.
- Moore Jr WH and Haynes WO. Alpha hemispheric asymmetry and stuttering: some support for a segmentation dysfunction hypothesis. *Journal of Speech and Hearing Research*, 23: 229–247, 1980.
- Nakata H, Sakamoto K, Ferretti A, Gianni Perrucci M, Del Gratta C, Kakigi R, et al. Somato-motor inhibitory processing in humans: an event-related functional MRI study. *NeuroImage*, 39: 1858–1866, 2008.
- Namasivayam AK and van Lieshout P. Investigating speech motor practice and learning in people who stutter. *Journal of Fluency Disorders*, 33: 32–51, 2008.
- Neumann K, Euler HA, von Gudenberg AW, Giraud AL, Lanfermann H, Gall V, et al. The nature and treatment of

- stuttering as revealed by fMRI a within- and between-group comparison. *Journal of Fluency Disorders*, 28: 381–409. quiz 409–410, 2003.
- Ning N, Lu C, Ma Z, Peng D, and Ding G. The speech planning deficit of people who stutter: evidence from word length effect. *Acta Psychologica Sinica*, 39: 215–224, 2007.
- Oldfield RC. The assessment and analysis of handedness: the Edinburgh inventory. *Neuropsychologia*, 9: 97–113, 1971.
- Packman A, Code C, and Onsjow M. On the cause of stuttering: integrating theory with brain and behavioral research. *Journal of Neurolinguistics*, 20: 353–362, 2007.
- Parent A. *Carpenter's Human Neuroanatomy*. Baltimore: Williams & Wilkins, 1996.
- Poulet JFA and Hedwig B. New insights into corollary discharges mediated by identified neural pathways. *Trends in Neurosciences*, 30: 14–21, 2007.
- Preibisch C, Neumann K, Raab P, Euler HA, von Gudenberg AW, Lanfermann H, et al. Evidence for compensation for stuttering by the right frontal operculum. *NeuroImage*, 20: 1356–1364, 2003.
- Rüsch N, Spoletini I, Wilke M, Bria P, Di Paola M, Di Iulio F, et al. Prefrontal-thalamic-cerebellar gray matter networks and executive functioning in schizophrenia. *Schizophrenia Research*, 93: 79–89, 2007.
- Rauschecker JP and Tian B. Processing of “what” and “where” in auditory association cortex. *International Congress Series*, 1250: 37–51, 2003.
- Remy F, Wenderoth N, Lipkens K, and Swinnen SP. Acquisition of a new bimanual coordination pattern modulates the cerebral activations elicited by an intrinsic pattern: an fMRI study. *Cortex*, 44: 482–493, 2008.
- Riley GD. *Stuttering Severity Instrument for Children and Adults*. Austin, TX: Pro-Ed, 1994.
- Saint-Cyr JA. Frontal–striatal circuit functions: context, sequence, and consequence. *Journal of the International Neuropsychological Society*, 9: 103–127, 2003.
- Salmelin R, Schnitzler A, Schmitz F, and Freund HJ. Single word reading in developmental stutterers and fluent speakers. *Brain*, 123: 1184–1202, 2000.
- Schlosser RG, Wagner G, and Sauer H. Assessing the working memory network: studies with functional magnetic resonance imaging and structural equation modeling. *Neuroscience*, 139: 91–103, 2006.
- Scott SK, Blank CC, Rosen S, and Wise RJ. Identification of a pathway for intelligible speech in the left temporal lobe. *Brain*, 123: 2400–2406, 2000.
- Smits-Bandstra S and De Nil LF. Sequence skill learning in persons who stutter: implications for cortico-striato-thalamo-cortical dysfunction. *Journal of Fluency Disorders*, 32: 251–278, 2007.
- Sommer M, Koch MA, Paulus W, Weiller C, and Buchel C. Disconnection of speech-relevant brain areas in persistent developmental stuttering. *Lancet*, 360: 380–383, 2002.
- Specht K and Reul J. Functional segregation of the temporal lobes into highly differentiated subsystems for auditory perception: an auditory rapid event-related fMRI-task. *NeuroImage*, 20: 1944–1954, 2003.
- Steiger JH and Lind JM. Statistically based tests for the number of common factors. In Paper Presented at the Annual Meeting of the Psychometric Society, Iowa City, IA, 1980.
- Takada M, Tokuno H, Nambu A, and Inase M. Corticostriatal input zones from the supplementary motor area overlap those from the contra- rather than ipsilateral primary motor cortex. *Brain Research*, 791: 335–340, 1998a.
- Takada M, Tokuno H, Nambu A, and Inase M. Corticostriatal projections from the somatic motor areas of the frontal cortex in the macaque monkey: segregation versus overlap of input zones from the primary motor cortex, the supplementary motor area, and the premotor cortex. *Experimental Brain Research*, 120: 114–128, 1998b.
- Tan L, Laird A, Li K, and Fox P. Neuroanatomical correlates of phonological processing of chinese characters and alphabetic words: a meta-analysis. *Human Brain Mapping*, 25: 83–91, 2005.
- van der Graaf FHCE, de Jong BM, Maguire RP, Meiners LC, and Leenders KL. Cerebral activation related to skills practice in a double serial reaction time task: striatal involvement in random-order sequence learning. *Cognitive Brain Research*, 20: 120–131, 2004.
- Watkins KE, Smith SM, Davis S, and Howell P. Structural and functional abnormalities of the motor system in developmental stuttering. *Brain*, 131: 50–59, 2008.
- WHO. Mental and behavioural disorders. In: International Statistical Classification of Diseases, 10th Revision (icd-10). 2nd ed. Geneva: World Health Organization, 2007.
- Wu JC, Maguire G, Riley G, Fallon J, LaCasse L, Chin S, et al. A positron emission tomography [18f]deoxyglucose study of developmental stuttering. *Neuroreport*, 6: 501–505, 1995.
- Xiong J, Gao JH, Lancaster JL, and Fox PT. Clustered pixels analysis for functional MRI activation studies of the human brain. *Human Brain Mapping*, 3: 287–301, 1995.
- Zhang Q and Yang Y. The determiners of picture-naming latency. *Acta Psychologica Sinica*, 35: 447–454, 2003.
- Zhuang J, LaConte S, Peltier S, Zhang K, and Hu X. Connectivity exploration with structural equation modeling: an fMRI study of bimanual motor coordination. *NeuroImage*, 25: 462–470, 2005.